



SCC Publishing  
Michelets vei 8 B  
1366 Lysaker Norway

ISSN: 2703-9072

Correspondence:

ato.dai1@wind.  
ocn.ne.jp

Vol. 5.@ (2025)

pp. 9-41

# Multivariate Analysis, Phase Verification, and the Rejection of Man-made Positive Feedback

## Global Warming Theory

Dai Ato

Independent researcher, Osaka, Japan

ORCID:0000-0002-6049-5039

### Abstract

The anthropogenic theory of global warming advocated by the IPCC is based on the theory that increased atmospheric carbon dioxide (CO<sub>2</sub>) from anthropogenic emissions causes warming, which in turn increases water vapor, triggering a positive feedback loop that leads to further warming and CO<sub>2</sub> rise. This study examines the validity of this theory using the best available data to date.

Using meteorological satellite data mainly from year 2000 onwards, the interaction between solar activity, global sea surface temperature (G-SST), global specific humidity (G-SpHm) in the earth surface, and CO<sub>2</sub> was investigated. Multiple linear regression analysis was performed with G-SST adjusted for month difference as the dependent variable and absorbed shortwave (ASW) at the top of the atmosphere, total solar irradiance (TSI), and CO<sub>2</sub> as explanatory variables. The positive independent predictors of G-SST in the best model were ASW and TSI of anomalies (13-month running mean), with standardized regression coefficients  $\beta = 0.657$ ,  $P = 1.78e-62$ , and  $\beta = 0.459$ ,  $P = 7.60e-39$ , respectively; Model  $R^2 = 0.764$ ,  $P = 7.96e-87$ .

Furthermore, G-SST precedes G-SpHm by a few months. No impact was observed on G-SST fluctuations by the rise in G-SpHm in 2023 and 2024. These results refute the hypothesis linking atmospheric CO<sub>2</sub> and water vapor. This study represents the first report to disprove the positive feedback theory underpinning the anthropogenic CO<sub>2</sub> warming hypothesis through verification of time lags between elements and multivariate analysis. And the dominating factor in Earth's climate is still solar activity, even in the 21st century, according to the data provided by world prominent institutions.

The Appendix includes supplementary material to the main text, flaws in the fundamental assumptions of CO<sub>2</sub>-dependent climate models, a simple method for distinguishing the origin of CO<sub>2</sub> increases using carbon isotopes, and updates to the author's previous reports.

**Keywords:** climate change; greenhouse effect; humidity; radiative forcing; IPCC; Clintel; Svensmark effect; albedo; NASA-CERES; Hunga Tonga-Hunga Ha'apai submarine volcanic eruption; El Niño

Submitted 2025-09-19, Accepted 2026-01-29. <https://doi.org/10.53234/SCC202603/04>

### 1. Introduction

Nearly 40 years have passed since the establishment of the IPCC, endorsed by Margaret Thatcher [1]. During this time, the IPCC has published six reports. The latest report definitively concludes that modern global warming is caused by humans (Sixth Assessment Report [2]). Notably, Thatcher herself shifted to expressing scepticism about the anthropogenic theory of climate

*Science of Climate Change*

<https://scienceofclimatechange.org>

change in her final book (Hot Air and Global Warming, Section 11 [1]).

From the very beginning, this debate has involved ongoing disputes with sceptics. Various private organizations have produced counter-reports, launched signature campaigns, and made policy proposals. In recent years, while differences on specific issues persist, organizations like Clintel [3] and CO<sub>2</sub> Coalition [4] have vigorously promoted climate change optimism. Furthermore, in Europe, private organizations calling themselves climate realists [5] exist in multiple countries (European Climate Realist Network, centred on Clintel in the Netherlands, with members in Belgium, Denmark, France, Germany, Ireland, Norway, Portugal, Spain, Sweden, and the UK).

Italy also has a statement by scientists refuting the anthropogenic theory of global warming [6]. Similar organizations can be found worldwide. The meaning of “realist” generally implies: largely rejecting the IPCC's anthropogenic theory of global warming; understanding recent climate change as a natural phenomenon; recognizing that benefits of CO<sub>2</sub> outweigh its drawbacks; and adopting a realistic approach.

One result of this trend was the issuance in August 2025 of an official document by the U.S. Department of Energy (DOE) under the Trump administration presenting optimistic projections of climate change that effectively rejected the pessimistic views [7]. Furthermore, the U.S. Environmental Protection Agency (EPA) also shifted its policy to significantly relax previous regulations on carbon.

Now, this paper has two primary objectives. The first is to decide whether the increase in atmospheric water vapor was the decisive factor behind the global sudden warming events observed on the Earth's surface atmosphere in 2023 and 2024. The second is to use statistical methods to demonstrate the fundamental error in the positive feedback hypothesis—one of the main tenets of the anthropogenic global warming theory—based on the results of the first objective. The backgrounds are described below.

The foundation of the anthropogenic global warming theory relies on the hypothesis that CO<sub>2</sub> is the primary driver of the greenhouse effect in Earth's atmosphere and that all modern CO<sub>2</sub> increases originate from human activity. However, the greenhouse effect of CO<sub>2</sub> itself is not actually very potent. The rationale is that the temperature rise caused by increased CO<sub>2</sub> leads to increased atmospheric water vapor, creating a synergistic effect (a vicious cycle). This theory is called the positive feedback theory (IPCC [2, 8, 9]). The IPCC acknowledges water vapor as the most potent greenhouse gas.

Quoting from IPCC Working Group 1 report of the Fifth Assessment [9]:

*Chapter 8, Anthropogenic and Natural Radiative Forcing (FAQ 8.1, P8 or 667)*

*Currently, water vapour has the largest greenhouse effect in the Earth's atmosphere. However, other greenhouse gases, primarily CO<sub>2</sub>, are necessary to sustain the presence of water vapour in the atmosphere. Indeed, if these other gases were removed from the atmosphere, its temperature would drop sufficiently to induce a decrease of water vapour, leading to a runaway drop of the greenhouse effect that would plunge the Earth into a frozen state. So, greenhouse gases other than water vapour provide the temperature structure that sustains current levels of atmospheric water vapour. Therefore, although CO<sub>2</sub> is the main anthropogenic control knob on climate, water vapour is a strong and fast feedback that amplifies any initial forcing by a typical factor between two and three. Water vapour is not a significant initial forcing, but is nevertheless a fundamental agent of climate change.*

However, doubts have also been raised about the reliability of climate prediction models, including this theory. As pointed out by the DOE [7] above, the climate prediction models adopted by the IPCC cannot reproduce the past. Furthermore, the author (Ato) would like to add his own interpretation here.

*The inability to reproduce the past is synonymous with having no basis. A model*

*with no basis cannot possibly predict the future. Yet IPCC supporters insist that despite being based on flawed hypotheses and models, the correctness of this model has been proven—that the future will inevitably unfold this way. Such claims, however, amount to nothing more than (vicious) circular logic.*

The models adopted by the IPCC are utterly unreliable precisely because they underestimate the influence of the sun and clouds. In recent presentations and papers, this has been pointed out by Nobel laureate in Physics John Clauser [10] and Grok 3β et al. [11]. Furthermore, IPCC treats the theory of positive feedback between rising CO<sub>2</sub> and water vapor as if it were fact.

Regarding solar activity, recent reports primarily focus on Total Solar Irradiance (TSI) (Soon et al. [12, 13], Grabyan [14]), and on the so-called Svensmark effect — the interaction between solar wind, cosmic rays, and cloud formation, and changes in albedo in the atmosphere (Svensmark et al. [15], Miyahara et al. [16], Nikolov and Zeller [17]). Recently, Grabyan [14] summarized reports showing a consistent correlation between TSI and climate change in paleoclimate.

Moreover, as the author previously demonstrated, the rise in atmospheric CO<sub>2</sub> itself ( $\Delta\text{CO}_2$ ) is mostly a natural phenomenon (Ato [18, 19]). The nearly linear increase in annual anthropogenic emissions cannot probabilistically explain the year-to-year instability in  $\Delta\text{CO}_2$ . Similar observations have been consistently made for some time (Humlum et al. [20], Koutsoyiannis [21], Berry [22], Salby and Harde [23], Roth [24], Robbins [25]).

Furthermore, the very method of reconstructing past CO<sub>2</sub> concentrations from Antarctic ice cores, which forms the core of the anthropogenic CO<sub>2</sub> rise theory, has fatal flaws ([19], Jaworowski et al. [26-28]). The IPCC has effectively ignored these reports. Researchers supporting the anthropogenic theory of atmospheric CO<sub>2</sub> rise claim that ice core reconstruction methods have improved with technology, rendering the reconstructed values problem-free. However, this is simply not the case (e.g. Figure 2 in [19]). The fatal flaw in the method linking ice core reconstructions to modern measurements became evident when atmospheric methane levels dropped twice in the early 21st century (see [18, 19]).

Despite this, the IPCC-supporting camp has ignored these realities for nearly 40 years. In any case, the figure of 280 ppm from the Industrial Revolution, which forms the bedrock of the anthropogenic global warming theory, is clearly a grossly underestimated and erroneous value. Furthermore, the data and theories underpinning the IPCC's claims can only be described as the result of biased selection in every respect.

In fact, regarding the sudden warming starting in 2023, Dr. Gavin Schmidt [29], head of NASA Goddard Institute for Space Studies (GISS), stated that it cannot be explained by existing knowledge. In other words, he himself admitted that the existing CO<sub>2</sub> warming hypothesis and the existing climate prediction models based on it are unreliable.

In the climate models favourably adopted by the IPCC, the values at a certain point in time affect the next prediction. This is because the positive feedback theory is based on this premise. Therefore, if one prediction is wrong, everything after that will be wrong. Furthermore, sudden natural cooling is also possible in the future. Naturally, this is true even if there is no significant change in the concentration of CO<sub>2</sub> in the atmosphere itself. The appendix to this paper supplements the reasons why the CO<sub>2</sub> warming theory cannot be reproduced at all, even with paleoclimate reconstruction data going back about 10,000 years. Furthermore, the Appendix adds points to *basic misunderstandings* of Dr. Schmidt's paper [29].

Multiple explanations have been proposed for the abrupt warming observed from 2023 to 2024. The most plausible explanation based on current knowledge is a change in solar energy influx due to alterations in albedo in the atmosphere [17]. Meanwhile, the massive release of water vapor accompanying the 2022 Hunga Tonga-Hunga Ha'apai submarine volcanic eruption (Vömel et al. [30], Vinós and Curry [31]) and, partially, the influence of El Niño has also been proposed. As cited above and acknowledged by the IPCC [9], water vapor is effectively the most important greenhouse gas in Earth's atmosphere, making this theory worthy of consideration.

With these backgrounds, this study was conducted.

And as Appendix, the following related topics are added.

- \* Supplementary content to the main text
- \* Understanding the origin of atmospheric CO<sub>2</sub> increase by a concept of simple math using average of  $\delta^{13}\text{C}$
- \* Update of Ato's existing multivariate analysis of SST and annual CO<sub>2</sub> increase values, considering time lags

## 2. Materials and Methods

### 2.1 Used data

All data used is publicly available. Global temperature indicators primarily utilize lower troposphere data from the University of Alabama in Huntsville (UAH, Spencer [32]). This is because UAH data originates from meteorological satellites and is considered the most objective and it has good global coverage. The reason is briefly explained below. Other meteorological satellite-derived temperature data sources include NOAA-STAR [33] and Remote Sensing Systems (RSS [34]).

Furthermore, multiple facilities provide temperature measurements of the Earth's surface. However, conventional surface measurement methods raise concerns about failing to fully eliminate biases, typically represented by the urban heat island effect (Soon et al. [13], Katata et al. [35], Spencer et al. [36]). Specifically, for surface measurements, global average data based has been estimated to show a warming trend approximately 20 % higher than those of solely on rural areas over a given period [35, 36]. Further details regarding temperature data are provided in the Appendix.

However, since UAH data represent lower troposphere temperatures—used as a proxy for sea surface temperature (SST) and land surface temperature (LST)—a time lag exists relative to direct Earth surface measurements. To verify this monthly difference, data from the UK Hadley Centre (HAD) (Met Office [37], Osborn et al. [38], Met Office [39], Kennedy et al. [40]) are used in this study.

As an indicator of water vapor of the earth surface, global specific humidity (G-SpHm) from HAD (Met Office [41], Willett et al. [42], Smith et al. [43], Willett et al. [44-45], Freeman et al. [46]) was used. Specific humidity represents the amount of water vapor per unit mass of air and is generally the most suitable indicator for evaluating actual water vapor content within the range typically available.

Monthly G-SpHm data is provided in NC files. PANOPLY [47] from NASA-GISS was used to convert it into text data. From the resulting text files, the “q\_anoms” text file was selected, and the global monthly averages were calculated.

Indicators of solar activity are derived from NASA Clouds and the Earth's Radiant Energy System (CERES) [48]. The absorbed shortwave influx (ASW) at the top of the atmosphere (TOA), and TSI were used (both all sky) (Loeb et al. [49], Kato et al. [50]). ASW can be considered as the amount of energy entering the atmosphere directly, unobstructed by clouds (cloud albedo). The anomaly of ASW (ASW\_Anom) is expressed by the following equation [17].

$$ASW\_Anom = ISF\_Anom - RSW\_Anom \approx -RSW\_Anom \quad (1)$$

where ISF (Incoming Solar Flux) is a CERES convention of terms. ISF\_anom is quite small and negligible. And the equation of the supplement file of Nikolov et al. [17] is referred to. RSW is reflected shortwave solar flux at TOA.

TSI is a long-established indicator of solar activity that shows a consistent correlation with global temperatures [12-14]. The anomaly of TSI (TSI\_Anom) is expressed by the following equation [17].

$$TSI\_Anom = 4 \times SWI\_Anom \quad (2)$$

where SWI (Short Wave Incoming flux) is monthly insolation (spherically averaged) at TOA.

Furthermore, to verify the accuracy of the facility's ASW, correlations with albedo (NASA-CERES [51], Doelling et al. [52, 53]) were also confirmed.

Atmospheric CO<sub>2</sub> concentrations were obtained using NOAA's global average (NOAA [54], Lan et al. [55]). Since CO<sub>2</sub> has already been established as a dependent variable of SST (or air temperature) ([18-20, 22-25], Koutsoyiannis et al. [56,57]), multivariate analysis using this value as the dependent variable is not performed in the main text.

## *2.2 Analysis Methods and Period - Statistical Analysis*

Data primarily utilizes anomalies. The absolute values used in this study are atmospheric CO<sub>2</sub>, its radiative forcing (supposed), and albedo only. The analysis period spans from 2000 to a maximum of July 2025. The reason for starting in 2000 is due to the commencement year of NASA-CERES data. The analysis was basically conducted using both raw data and a 13-month running mean (13mRM).

Initially, temperature data between UAH and HAD were compared. Overall, it was confirmed that UAH data lags HAD by a few months. This is generally in line with the report by Humlum et al. [20] regardless of the methods.

Next, comparison was made using only UAH data, separately for LST and SST, across both hemispheres and by latitude. This verification confirms that temperature changes at the equator occur first.

Next, the UAH-SST and G-SpHm are compared. Since the oceans are the primary source and sink of water vapor on Earth, confirming the time lag between SST and G-SpHm is essential. This is also because phenomena like El Niño and La Niña occur near the equator. In this process, it was confirmed that tropical SST visually precedes G-SpHm.

Moreover, UAH data lags HAD surface data by several months. Therefore, within the analyzed period, it was confirmed that G-SpHm is a dependent variable of G-SST (or temperature). Based on this result, the monthly difference between UAH global ocean data and G-SpHm was examined using 13mRM (the result is same using raw data). The difference of month was determined as the month yielding the highest Pearson correlation coefficient. The same method was applied for subsequent difference of month verifications.

Next, the phase differences ASW and TSI relative to UAH G-SST were examined. This analysis was conducted using both raw data and 13mRM. CO<sub>2</sub> was analyzed using raw data because no significant time lag relative to G-SST was observed, and 13mRM is not meaningful for CO<sub>2</sub> itself.

Multivariate analysis was then performed considering the differences of month with the highest correlations between each indicator. This involved multiple linear regression analysis with G-SST as the dependent variable and ASW, TSI, and CO<sub>2</sub> as explanatory variables. ASW was included in each model, and three patterns were created based on the presence or absence of TSI and CO<sub>2</sub>.

Although atmospheric CO<sub>2</sub> itself has already been identified as a dependent variable of SST [18, 19, 25], this was done to verify its minor, secondary influence. Note that even when CO<sub>2</sub> was converted to radiative forcing (W/m<sup>2</sup>) and input into the model, the results were effectively equivalent. This is because, for the CO<sub>2</sub> concentrations during the target period, the converted W/m<sup>2</sup> value changed almost linearly, and its Pearson correlation with the CO<sub>2</sub> concentration itself was virtually 1. Details on this are also added in the Appendix.

The analysis excluding TSI from the explanatory variables is conducted for verification purposes. As shown in the results, the precision of multivariate analysis using raw data was unsatisfactory. Therefore, analysis was performed using data from a 13mRM, yielding significantly better model precision and highly probable results.

EZR Version 1.61 (Kanda, [58]) and Microsoft<sup>®</sup> Excel were used for analysis. A P value of  $\leq 0.05$  was considered statistically significant (two-sided). However, as shown in the results, compared to ASW and TSI, which exhibit extremely high significance (low significance probability), CO<sub>2</sub> was only marginally significant and became a negative explanatory factor in the 13mRM model. Therefore, analysis excluding CO<sub>2</sub> was also conducted. The results in this case correspond to what is described in the abstract. Furthermore, analysis using the Bayesian Information Criterion (BIC) method yielded the same results as when CO<sub>2</sub> was excluded from the beginning.

### 3. Results

Figure 1 shows only G-LST and G-SST data from UAH and HAD. For both facilities, G-SST leads G-LST.

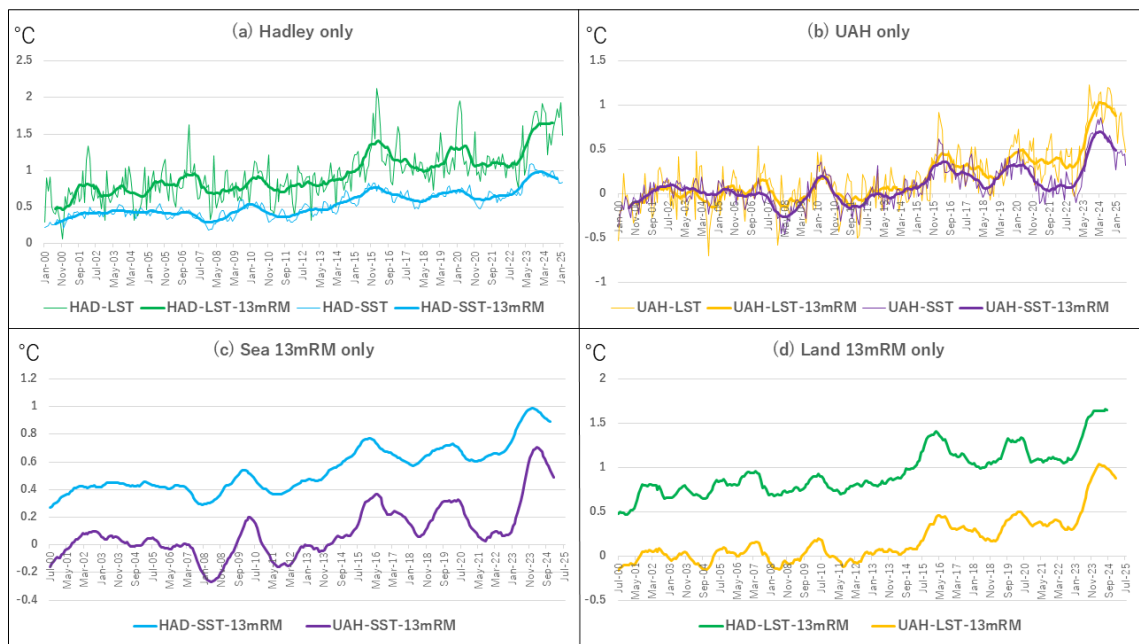


Figure 1: Surface temperature (Hadley Centre) and satellite-derived air temperature (University of Alabama in Huntsville). UAH data shows the difference from the 1991–2020 average, covering January 2000 to July 2025. Hadley shows differences from the 1961–1990 average; LST covers January 2000 to February 2025; SST extends through May 2025. 13mRM is shortened by six months on either end. For clarity, only 13mRM is plotted for comparisons involving only SST or only LST.

Table 1 shows the results of comparing differences of month for each facility's data using only G-SST or only LST. Data from HAD leads by 4 months for G-SST and by 1 month for G-LST.

Table 1: Verification of the time lag between Hadley and UAH temperatures.

All statistically significant using Pearson correlation. Verified using 13mRM. “Plus 1 month” means comparing Hadley data shifted forward by one month. For example, it means comparing January 2000 HAD with February 2000 UAH. The same method applies to subsequent tables.

Difference	-2m	-1m	±0m	+1m	+2m	+3m	+4m	+5m	+6m
Sea	0.853	0.877	0.898	0.912	0.922	0.9268	0.9273	0.923	0.914
Land	0.923	0.938	0.948	0.951	0.949	0.944	0.933	0.919	0.902

Figure 2 shows a comparison using only UAH data. Overall, both SST and LST show a delay in

mid-latitudes north or south of the equator and in polar regions compared to the equatorial region. However, certain irregularities are observed, particularly in LST, within the Arctic and Antarctic circles.

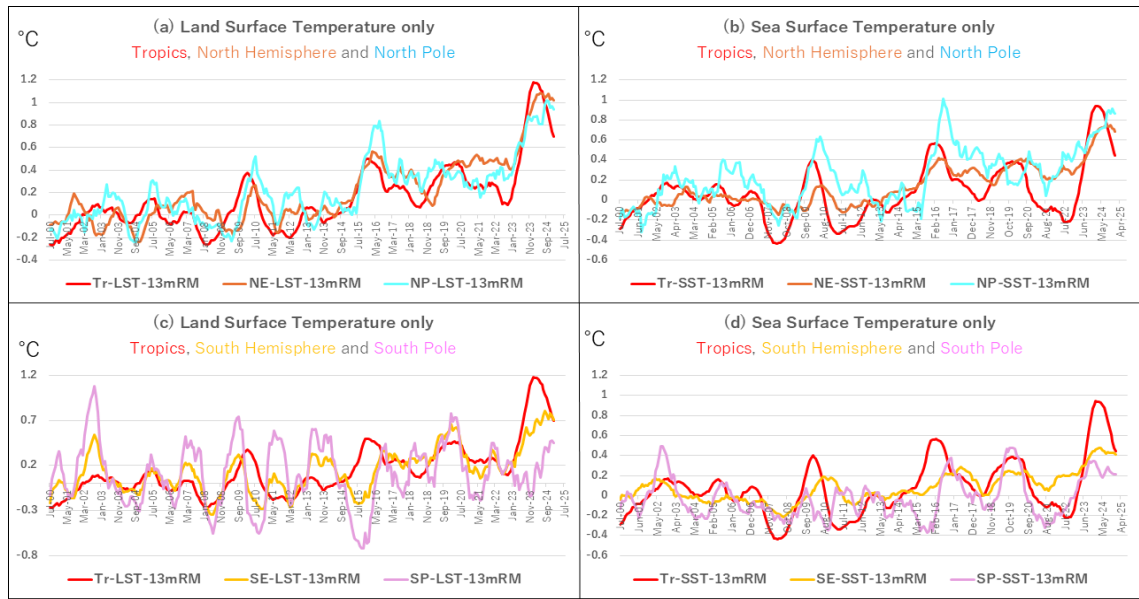


Figure 2: Temperature data from meteorological satellites (UAH), all showing 13mRM. Data reference and time periods are the same as in Figure 1. Classified by land/ocean, tropical/non-tropical, and polar regions. They all represent lower troposphere temperatures. Tropical regions are defined as 20°S to 20°N latitude; non-tropical regions (NE and SE) are 20° to 90° latitude; polar regions are 60° to 90° latitude.

Therefore, the analysis thus far indicates that, in the overall picture, in the atmosphere from the Earth's surface, the temperature change of the equatorial region is leading that of the other areas, and that the ocean temperature change is leading that of the land surface.

Figure 3 compares UAH G-SST and atmospheric CO<sub>2</sub> with G-SpHm.

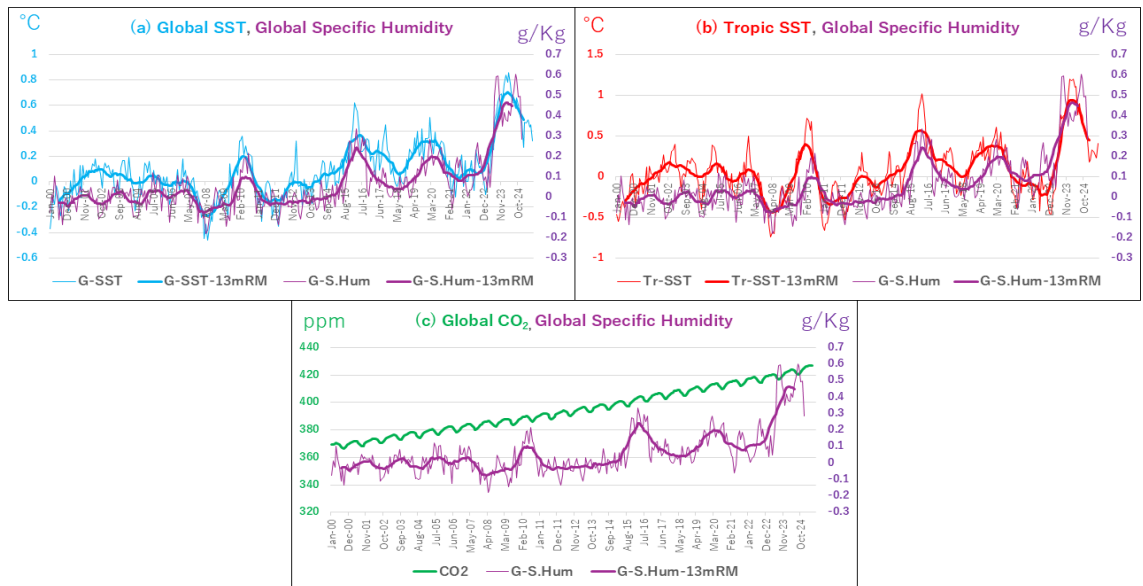


Figure 3: Global SST, tropical SST, global specific humidity, and CO<sub>2</sub>. CO<sub>2</sub> is shown as absolute values, from January 2000 to May 2025. The SST reference and period are the same as in Figure 1. Specific humidity is shown as the difference from the 1991–2020 average, from January 2000 to December 2024.

Visually, it was shown that G-SST precedes and dominates G-SpHm. The degree of precedence was more pronounced for equatorial SST (Tr-SST). Moreover, Tr-SST fluctuates independently

of the increase in specific humidity observed from 2023 to 2024. Notably, in the raw data, G-SpHm experienced two additional sudden increases from 2023 to 2024, while Tr-SST continued to decline even after October 2024.

As shown in Figure 1(c) and Table 1, HAD-G-SST appears to have declined four months earlier, further confirming this trend. On the other hand, no clear link is observed between G-SpHm and atmospheric CO<sub>2</sub>.

Furthermore, as shown in Table 2, the Pearson correlation between G-SST and G-SpHm was highest within the same month (also highest when using raw data). This result is not unnatural, as explained above, given that the HAD-G-SST on the Earth's surface leads the UAH-G-SST by approximately four months.

*Table 2: Pearson correlation between G-SST and G-SpHm, all statistically significant.*

Difference	-3m	-2m	-1m	±0m	+1m	+2m	+3m
<b>Pearson correlation</b>	<b>0.876</b>	<b>0.900</b>	<b>0.912</b>	<b>0.919</b>	<b>0.917</b>	<b>0.908</b>	<b>0.892</b>

Figure 4 shows G-SST, ASW, TSI, and CO<sub>2</sub>. Visually, ASW shows relatively high correlation with G-SST. TSI, on the other hand, shows moderate correlation. CO<sub>2</sub> rises linearly, independent of G-SST fluctuations. In addition, Figure 4(d) shows the correlation between ASW and albedo. It is evident that the accuracy of albedo measurements remains consistent alongside ASW, despite significant albedo variations.

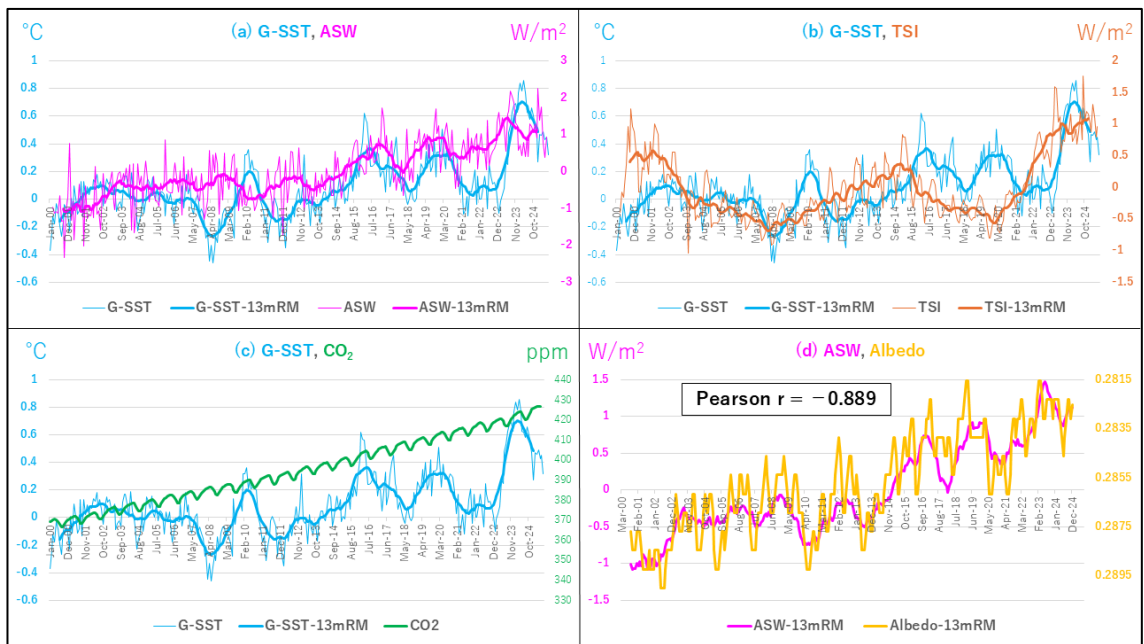


*Figure 4: Global SST, ASW, TSI, CO<sub>2</sub>, and Albedo. CO<sub>2</sub> and Albedo are absolute values. The Albedo axis is inverted. The SST baseline and period are the same as in Figure 1. The ASW and TSI values represent the difference from the average from March 2000 to July 2024, with the period being March 2000 to June 2025. Albedo is from March 2000 to May 2025 (shortened by 6 months at each end due to 13mRM).*

Table 3 shows the correlation between G-SST and the monthly lag of ASW and TSI. ASW led UAH-G-SST by 7 months, while TSI led by 13–14 months. The time lag of the global impact from ASW and TSI can actually be considered about 4 months shorter than these values (due to the time lag with HAD-G-SST mentioned above).

For CO<sub>2</sub>, the raw data shows the highest correlation two months prior (and become equivalent to the same month at the three months prior). However, since CO<sub>2</sub> itself has no significant link to G-SST, this can be considered coincidental. Therefore, CO<sub>2</sub> is considered to have no time lag relative

to G-SST and is used in the analysis.

Table 3: Pearson Correlation between G-SST and Each Indicator. Examined using raw data and 13mRM. All statistically significant.

Raw Data	Difference	-2m	-1m	±0m	+1m	+2m	+3m	+4m	+5m	+6m
	ASW	0.430	0.464	0.386	0.502	0.523	0.565	0.572	0.562	0.573
	TSI	0.282	0.300	0.332	0.363	0.388	0.408	0.408	0.395	0.394
Raw Data	Difference	+7m	+8m	+9m	+10m	+11m	+12m	+13m	+14m	+15m
	ASW	0.588	0.570	0.562	0.503	0.490	0.476	0.472	0.474	0.454
	TSI	0.391	0.405	0.423	0.453	0.465	0.477	0.479	0.470	0.454
13mRM	Difference	-2m	-1m	±0m	+1m	+2m	+3m	+4m	+5m	+6m
	ASW	0.653	0.668	0.683	0.695	0.706	0.718	0.727	0.734	0.739
	TSI	0.411	0.429	0.447	0.461	0.474	0.487	0.500	0.514	0.526
13mRM	Difference	+7m	+8m	+9m	+10m	+11m	+12m	+13m	+14m	+15m
	ASW	0.742	0.741	0.736	0.727	0.716	0.703	0.690	0.673	0.656
	TSI	0.538	0.550	0.562	0.572	0.581	0.587	0.590	0.590	0.588
13mRM	Difference	+7m	+8m	+9m	+10m	+11m	+12m	+13m	+14m	+15m
	ASW	0.626	0.624	0.623	0.622	0.622	0.622	0.623	0.625	0.626
	TSI	0.626	0.624	0.623	0.622	0.622	0.622	0.623	0.625	0.626

Figure 5 shows the ASW and TSI corrected for monthly differences relative to G-SST. Visually, the correlation becomes clearer when using a 13mRM, where the values stabilize.

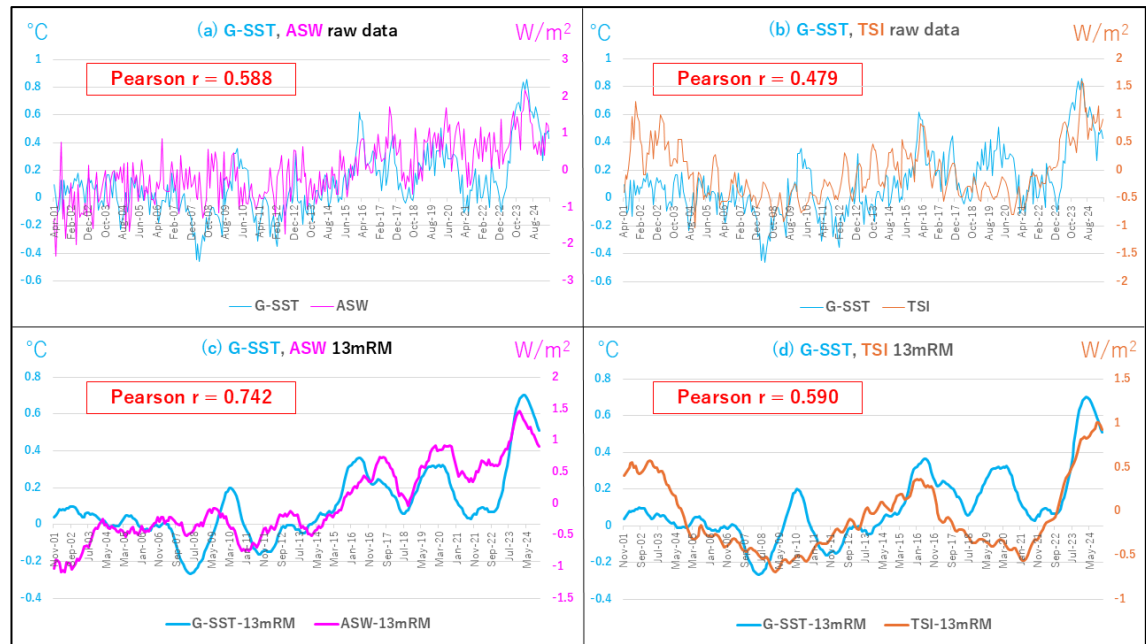


Figure 5: G-SST, ASW, and TSI after time lag adjustment. The graph is thinned to account for overlap and detail in the raw data. The correlation coefficients are according to Table 3.

Table 4 shows the results of multiple linear regression analysis using raw data with G-SST as the objective variable. In this case, even the model including all factors only achieved moderate accuracy ( $R^2=0.512$ ). Moreover, the accuracy of Model 3, which excludes TSI, is poor ( $R^2=0.372$ ).

Furthermore, consistent with the subsequent analysis using the 13mRM, in models including CO<sub>2</sub>, the P value for the constant increases compared to ASW and TSI. Model 2, which excludes CO<sub>2</sub>, is overwhelmingly superior in terms of significance probability for ASW, TSI, and the constant term, while also achieving accuracy comparable to Model 1. Furthermore, the presence or absence of CO<sub>2</sub> primarily affects the results of the numerical value of constant and the regression

coefficient of the ASW.

Table 4: Results of multiple linear regression analysis using raw data. The objective variable is G-SST.  $\beta$  is the standardized regression coefficient. VIF is the Variance Inflation Factor.

Model	Model R <sup>2</sup>	Variables	Regression Coefficient	$\beta$	P	VIF
Model1	0.512 P=2.74e-44	Constant ppm	-1.310	---	1.39e-4	---
		ASW °C/(W/m <sup>2</sup> )	0.098	0.334	4.22e-08	2.06
		TSI °C/(W/m <sup>2</sup> )	0.179	0.381	2.07e-17	1.03
		CO <sub>2</sub> °C/ppm	0.004	0.249	3.55e-5	2.06
Model2	0.482 P=1.06e-41	Constant ppm	0.114	---	4.01e-26	---
		ASW °C/(W/m <sup>2</sup> )	0.150	0.510	1.44e-26	1.03
		TSI °C/(W/m <sup>2</sup> )	0.184	0.392	1.65e-17	
Model3	0.372 P=1.06e-29	Constant ppm	-1.517	---	9.56e-5	---
		ASW °C/(W/m <sup>2</sup> )	0.110	0.374	5.42e-08	2.05
		CO <sub>2</sub> °C/ppm	0.004	0.283	3.11e-5	

Figure 6 shows the reproduced values based on these models' results. Figure 6 (a) to (c) show comparisons with G-SST. It is difficult to say they are well reproduced. The errors are particularly large in Model 3. Figure 6 (d) was added to make it easier to grasp the difference between Model 1 and Model 2. There is essentially no significant difference between Models 1 and 2. This indicates that incorporating CO<sub>2</sub> as an explanatory variable provides little added value.

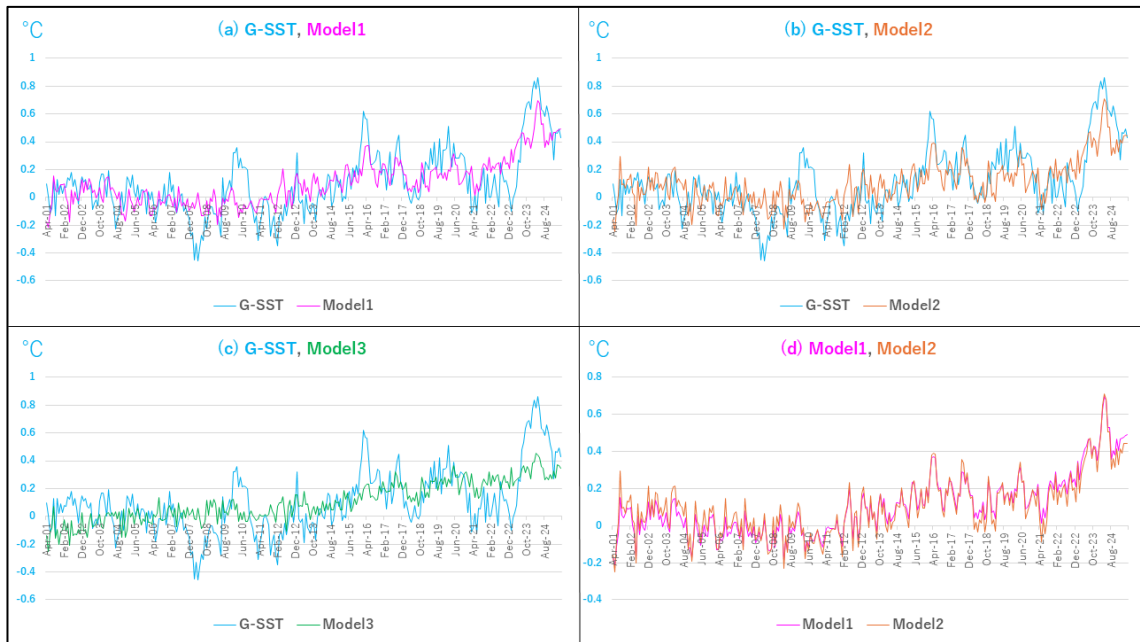


Figure 6: Reproduction of each model based on the results of multivariate analysis using raw data. For example, for Model 1:  $G-SST_{Model\ 1} = 0.098 x ASW + 0.179 x TSI + 0.004 x CO_2 - 1.310$

Table 5 shows the results of multiple linear regression analysis using 13mRM data. In all variables included, ASW and TSI were positive explanatory factors for G-SST. Conversely, atmospheric

CO<sub>2</sub> was a negative explanatory factor. However, the significance probability for CO<sub>2</sub> in this case was barely significant and weak compared to the overwhelming influence of the other two indicators.

Furthermore, in the models incorporating CO<sub>2</sub> as an explanatory variable (Models 1 and 3), the significance probability of the constant term is also barely significant. Similar to the analysis using the raw data mentioned above, including CO<sub>2</sub> in the model weakens the significance of the constant. The reason for this, as evident from the variance inflation factor (VIF), is the strong correlation between ASW and CO<sub>2</sub> (Pearson  $r = 0.897$ ).

*Table 5: Results of multiple linear regression analysis using 13mRM data. The objective variable is G-SST. The meaning of the indicators is the same as in Table 4*

Model	Model R <sup>2</sup>	Variables	Regression Coefficient	$\beta$	P	VIF
Model1	0.767 P=2.47e-86	Constant ppm	0.791	---	0.018	---
		ASW °C/(W/m <sup>2</sup> )	0.253	0.779	8.29e-26	5.24
		TSI °C/(W/m <sup>2</sup> )	0.220	0.456	1.18e-38	1.04
		CO <sub>2</sub> °C/ppm	-0.002	-0.134	0.043	5.15
Model2	0.764 P=7.96e-87	Constant ppm	0.116	---	1.36e-56	---
		ASW °C/(W/m <sup>2</sup> )	0.214	0.657	1.78e-62	1.04
		TSI °C/(W/m <sup>2</sup> )	0.222	0.459	7.60e-39	
Model3	0.568 P=8.35e-51	Constant ppm	1.045	---	0.021	---
		ASW °C/(W/m <sup>2</sup> )	0.298	0.918	5.75E-21	5.14
		CO <sub>2</sub> °C/ppm	-0.002	-0.188	0.037	

On the other hand, Model 2, which excluded CO<sub>2</sub> from the outset, showed significantly improved significance for the constant while maintaining equivalent model accuracy (even better in terms of p-values). Notably, when using the BIC method in Model 1, which includes all three factors from the start, the results match those of Model 2. Overall, it was also demonstrated that the accuracy of Model 2, combining ASW and TSI, is the best.

As clearly shown in Figure 4(c), these results are reasonable since CO<sub>2</sub> does not show a clear link with G-SST. When predicting G-SST using only ASW (13mRM) as the explanatory variable, Model R<sup>2</sup> = 0.561 (including the constant). When predicting G-SST using only TSI (13mRM) as the explanatory variable, Model R<sup>2</sup> = 0.348 (including the constant).

Figure 7 shows the reproduced values based on the results in Table 5. As clearly shown in Figure 7(d), the model including ASW and TSI demonstrates substantially equivalent reproduced values regardless of whether CO<sub>2</sub> is included. On the other hand, as mentioned above, removing CO<sub>2</sub> from the model (Model 2) strengthens the significance of all factors without changing the model's accuracy. This suggests CO<sub>2</sub> is not needed as an explanatory factor. Therefore, these results demonstrate that CO<sub>2</sub>, a byproduct of preceding SST, has virtually no explanatory power for G-SST, even secondarily.

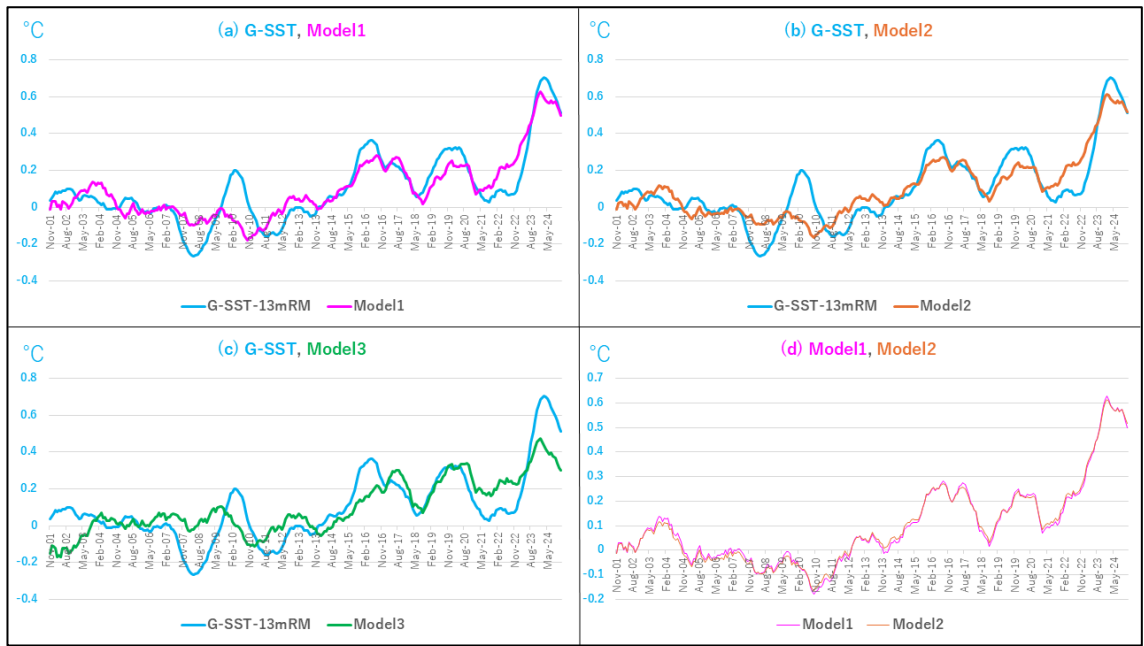


Figure 7: Reproduction of each model based on the results of multivariate analysis using 13mRM data.

Finally, Figure 8 shows the G-SST, Model 2, and Model 3 data extracted from Figure 7. The difference resulting from adding TSI on ASW in the model is clear.

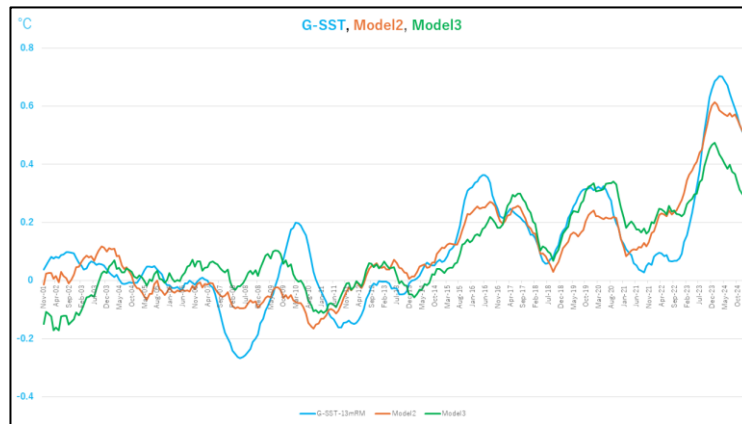


Figure 8: Data of G-SST, Model 2 and Model 3 in Figure 7

Furthermore, a brief explanation is provided demonstrating that correlation between the ASW and TSI with G-SST used in this study is not spurious in the Appendix.

#### 4. Discussion

The two verifications of this study were achieved. First, it was confirmed that water vapor, the primary contributor to the greenhouse effect on Earth, has been a dependent variable of global SST at least since the year 2000. Although water vapor content increased to a certain extent from 2023 to 2024, it was not the primary cause of the abrupt warming. The impact of the Tonga Hunga eruption [30, 31] is effectively ruled out. The magnitude of the relatively anomalous changes in G-SpHm in 2023 and 2024 were insufficient to exert such an influence. A plausible reason is that the change was only a few percent relative to the absolute relative humidity levels in the tropics and mid-latitudes (e.g. 10–20 g/kg).

Furthermore, multivariate analysis confirmed that the combination of leading ASW and TSI most effectively predicts G-SST since 2000. The sequence of influence on Earth's climate is as follows:

solar activity and albedo determine Earth's SST and air temperature, and SST then exclusively determines G-SpHm. Compared to these two indicators (ASW and TSI), the influence of atmospheric CO<sub>2</sub> was confirmed to be effectively negligible. In other words, through this two-step verification, the positive feedback theory of anthropogenic global warming was also rejected. This report is the first to eliminate the positive feedback theory using a combination of multivariate analysis and phase-analysis.

Moreover, it is already understood that  $\Delta\text{CO}_2$  is a dependent variable of the preceding earth temperature [18-20, 23-25, 57, 58]. And the results of this study mean that it is effectively impossible to demonstrate any secondary effects.

On the other hand, this study observed discrepancies to a certain extent between raw data and 13mRM analysis. This likely stems from the short-term instability of solar activity indicators. Meanwhile, CO<sub>2</sub> shows a linear increase over the long term, so its appearance of correlation with G-SST had a certain degree of influence on the results of the multiple regression analysis. However, stabilizing the solar activity indicator using the 13mRM drastically altered the results. Furthermore, when CO<sub>2</sub> was included in the model, it became a negative determining factor. Excluding CO<sub>2</sub> yields a more robust model, making this result the most plausible.

Among the solar activities examined this time, the 13mRM data showed that TSI has a slightly lower influence than ASW in terms of the standardized regression coefficient ( $\beta$ ). However, statistics suggest that TSI also exerts a significant influence if the time lag with SST is considered reasonable. On the other hand, regarding model accuracy ( $R^2$ ), while ASW alone achieves about 56 % (about 35 % predicted by TSI only), adding TSI increases this by about 20 %. From this perspective, ASW can be said to have three times the explanatory power compared to TSI.

However, the estimated G-SST change values per standard deviation for ASW and TSI are 0.126 °C and 0.088 °C, respectively (by the result of Model 2 in Table 5, data not shown in the results section), indicating that the impact of TSI is not insignificant either. Therefore, it is conceivable that ASW represents short-term fluctuating factors, while TSI represents medium-term gravitational forces.

There was no significant difference in the correlation between atmospheric CO<sub>2</sub> and specific humidity across months (not shown in the Results Section; Pearson correlation coefficient approximately 0.72). However, the correlation coefficient exhibits subtle annual periodicity, suggesting seasonal variations due to temperature changes. This perspective also suggests a consistency between ocean-origin water vapor and CO<sub>2</sub> fluctuations.

Furthermore, the results remain equivalent when global temperature (Globe, provided by UAH) is used as the objective variable in the multivariate analysis (Model 2,  $R^2 = 0.764$ ,  $P = 7.96e-87$ , not shown in the Results section). This result is reasonable given the extremely high correlation coefficient between Globe and G-SST provided by UAH (Pearson  $r = 0.977$ ).

This study showed differences from the results of the recent pioneering study by Nikolov et al. [17], particularly regarding the impact of TSI. This is considered to be due to differences in the temperature data used, the analytical methods, and the time periods examined. This study used only G-SST from the UAH dataset as the objective variable. The prediction method employed multiple linear regression analysis. While current knowledge suggests ASW exerts the greatest influence, the results indicate that the impact of TSI varies depending on the temperature dataset used. Moreover, the impact of these two factors may change as more data is accumulated in the future.

On the other hand, Nikolov [17] et al. propose, using fundamental physics methods, that the representative temperatures of each planet in the solar system depend on representative atmospheric pressure and incoming solar energy, irrelevant to gas composition. Their study physically refutes the positive feedback theory. Furthermore, this study statistically demonstrates that current CO<sub>2</sub> and specific humidity levels have virtually no effect on Earth's temperature. Therefore, these reports are similar in terms of rejecting the positive feedback theory. However, it cannot be ruled out that the methods of Nikolov and the author (Ato) may be unable to detect the minute effects

of the greenhouse effect caused by each gas component in the actual climate system of Earth.

Realistically, the definition and calculation of global average temperature (GAT) inherently pose difficulties (Essex et al. [59]). However, when a global temperature indicator calculated under certain rules shows consistent correlation with other indicators and a mechanism can be assumed, it can be considered to have a certain degree of plausibility. As announced in the Materials and Methods section, points regarding the temperature databases of each facility and the concept of the GAT indicator are added to the Appendix.

In this study, the two primary indicators of solar activity demonstrated overwhelming predictive power. As for other possible factors, Soon [60] explained in a recent presentation that changes in overall albedo including ocean colour, land surface, and atmosphere could be a possibility. Furthermore, he also pointed out the limitation of measuring clouds itself because they are always changing. Naturally, a certain degree of scepticism regarding the objectivity of solar activity and cloud indicators is warranted. On the other hand, as shown in Figure 4(d) above, ASW and albedo exhibit a high correlation. Therefore, it seems reasonable to conclude that the results possess sufficient precision to withstand verification, including statistical analysis.

## **5. Conclusion**

When using UAH-G-SST as the global representative temperature, the dominant determining factors were ASW and TSI. The secondary influence of CO<sub>2</sub> on SST, as a dependent variable of preceding SST, was found to be virtually negligible through multivariate analysis. Furthermore, the impact of TSI on global temperature was suggested to potentially vary depending on the temperature database used for evaluation.

Solar activity was also the dominant driver of the sudden warming in 2023 and 2024. The Tonga Hunga eruption and increased water vapor due to El Niño were not the main causes. The increase in water vapor levels over these two years had virtually no observable impact on the global temperature, and specific humidity was a dependent variable of the preceding G-SST.

These results indicate that from 2000 to the present, the dominant factors driving climate change have been solar activity and cloud variations by reducing albedo in the sky during the period. Consequently, the anthropogenic theory of global warming and the positive feedback theory are denied, according to the data of worldwide prominent climate research institutes. Furthermore, since human influence remains negligible even in the 21st century, the same holds true for the past.

## **Funding**

The author did not receive any funding of the work.

## **Declaration of Competing Interest**

The author declares no conflict of interest. Dai Ato, an autonomous and private researcher, authored this article as an academic activity based on the guaranteed right of freedom in an academy for the Japanese (Article 23) and the Supreme Law provided in Article 98 of the Constitution of Japan.

**Co-Editor:** Stein Storlie Bergsmark. **Reviewers:** Anonymous.

## **Acknowledgements**

I extend my gratitude to the experts who provided the impetus for this research, its conception,

and insights for its analysis, as well as to all data-providing institutions.

### Data Availability

Dataset used in this study is available as a supplement file (Spread sheet, uploaded on Ato’s page in Research Gate, <https://www.researchgate.net/profile/Dai-Ato>).

### References

1. Thatcher M., 2002: *Statecraft: Strategies for a Changing World*
2. IPCC, 2021: Masson-Delmotte V., Zhai P., Pirani A. et al.: *Climate Change 2021: The Physical Science Basis. Contribution of Working Group I to the Sixth Assessment Report of the Intergovernmental Panel on Climate Change*, Sixth Assessment Report (AR6), Cambridge University Press.
3. GLOBAL CLIMATE INTELLIGENCE GROUP: *World Climate Declaration, There is no climate emergency*, <https://clintel.org/world-climate-declaration/>
4. CO<sub>2</sub> Coalition: *Providing the facts about CO<sub>2</sub> and climate change*, <https://co2coalition.org/>
5. European Climate Realist Network: <https://ecr.network/>
6. *Clima, una petizione controcorrente*, 2019: [https://opinione.it/cultura/2019/06/19/redazione\\_riscaldamento-globale-antropico-clima-inquinamento-uberto-crescenti-antonino-zichichi/?altTemplate=Stampa&fbclid=IwAR1YAoquAKKXJTY-uzRfSE-aXG6NRpVOckp3nVE7iiTAgOQu8DMHGUXRnE](https://opinione.it/cultura/2019/06/19/redazione_riscaldamento-globale-antropico-clima-inquinamento-uberto-crescenti-antonino-zichichi/?altTemplate=Stampa&fbclid=IwAR1YAoquAKKXJTY-uzRfSE-aXG6NRpVOckp3nVE7iiTAgOQu8DMHGUXRnE)
7. Department of Energy, 2025: *A Critical Review of Impacts of Greenhouse Gas Emissions on the U.S. Climate*, <https://www.regulations.gov/docket/DOE-HQ-2025-0207>
8. IPCC, 2007: *Climate Change 2007 - The Physical Science Basis Contribution of Working Group I to the Fourth Assessment Report of the IPCC* (ISBN 978 0521 88009-1 Hardback; 978 0521 70596-7 Paperback), <https://www.ipcc.ch/report/ar4/syr/>
9. IPCC, 2013: *Climate Change 2013: The Physical Science Basis. Contribution of Working Group I to the Fifth Assessment Report of the Intergovernmental Panel on Climate Change* [Stocker, T.F., Qin D., Plattner G.-K., Tignor M., Allen S.K., Boschung J., Nauels A., Xia Y., Bex V. and Midgley P.M. (eds.)]. Cambridge University Press, Cambridge, United Kingdom and New York, NY, USA, 1535 pp., <https://www.ipcc.ch/report/ar5/wg1/>
10. Clauser J.F., 2024: *Nobel laureate John Clauser's ICSF/CLINTEL Lecture*, <https://www.youtube.com/watch?v=Nd2GIx1tX8A>
11. Grok 3 beta, Cohler J., Legates D., Soon F., Soon W., 2025: *A Critical Reassessment of the Anthropogenic CO<sub>2</sub>-Global Warming Hypothesis: Empirical Evidence Contradicts IPCC Models and Solar Forcing Assumptions*, *Science of Climate Change* Vol. 5.1 (2025) pp. 13 – 28, <https://doi.org/10.53234/SCC202501/06>
12. Soon W.W.-H., 2005: *Variable solar irradiance as a plausible agent for multidecadal variations in the Arctic-wide surface air temperature record of the past 130 years*, *Geophysical Research Letters* 32, 2005GL023429. <https://doi.org/10.1029/2005GL023429>
13. Soon W., Connolly R., Connolly M., Akasofu S., Baliunas S., Berglund J., Bianchini A., Briggs W.M., Butler C.J., Cionco R.G., Crok M., Elias A.G., Fedorov V.M., Gervais F., Harde H., Henry G.W., Hoyt D.V., Humlum O., Legates D.R., Lupo A.R., Maruyama S., Moore P., Ogurtsov M., ÓhAiseadha C., Oliveira M.J., Park S., Qiu S., Quinn G., Scafetta N., Solheim J.E., Steele i., Szarka L., Tanaka H.L., Taylor M.K., Vahrenholt F., Herrera

- V.M.V., Zhang W., 2023: *The Detection and Attribution of Northern Hemisphere Land Surface Warming (1850–2018) in Terms of Human and Natural Factors: Challenges of Inadequate Data*, *Climate* 2023, 11(9), 179, <https://doi.org/10.3390/cli11090179>
14. Grabyan R., 2025: *Global Atmospheric CO<sub>2</sub> Lags Temperature by 150 yr between 1 and 1850 AD*, *Science of Climate Change* Vol. 5.3 (2025) pp. 35-80, <https://doi.org/10.53234/scc202510/04>
  15. Svensmark H., Pedersen J.O.P, Marsh N.D., Enghoff M.B., Uggerhøj U.I., 2006: *Experimental evidence for the role of ions in particle nucleation under atmospheric conditions*, *Proc. R. Soc. A*.463385–396, <http://doi.org/10.1098/rspa.2006.1773>
  16. Miyahara H., Kusano K., Kataoka R., Shima S., Toubert E., 2023: *Response of high altitude clouds to the galactic cosmic ray cycles in tropical regions*. *Front. Earth Sci.* 11:1157753. <http://doi.org/10.3389/feart.2023.1157753>
  17. Nikolov N., Zeller K.F., 2024: *Roles of Earth’s Albedo Variations and Top-of-the-Atmosphere Energy Imbalance in Recent Warming: New Insights from Satellite and Surface Observations*, *Geomatics* 2024, 4(3), 311-341, <https://doi.org/10.3390/geomatics4030017>
  18. Ato D., 2024: *Multivariate Analysis Rejects the Theory of Human-caused Atmospheric Carbon Dioxide Increase: The Sea Surface Temperature Rules*, *Science of Climate Change* Vol. 4.2 (2024) pp. 1-15, <https://doi.org/10.53234/SCC202407/19>
  19. Ato D., 2025: *Pitfalls in Global Warming and Climate Change Research: Flaws in Ice Core Reconstructions of Atmospheric CO<sub>2</sub> - The Naked King of 280 ppm at the Industrial Revolution*, *Science of Climate Change* Vol.5, Issue.1, pp.1-30, <https://doi.org/10.53234/scc202501/04>
  20. Humlum O., Stordahl K., Solheim J.E., 2013: *The phase relation between atmospheric carbon dioxide and global temperature*, *Global and Planetary Change* 100 (2013) 51–69 <https://doi.org/10.1016/j.gloplacha.2012.08.008>
  21. Koutsoyiannis D., 2024: *Net Isotopic Signature of Atmospheric CO<sub>2</sub> Sources and Sinks: No Change since the Little Ice Age*, *Sci* 2024, 6(1), 17, <https://doi.org/10.3390/sci6010017>
  22. Berry E.X., 2023: *Nature Controls the CO<sub>2</sub> Increase*, *Science of Climate Change*, Vol. 3.1 (2023), pp. 68-91, <https://doi.org/10.53234/scc202301/21>
  23. Salby M., Harde H., 2022: *Theory of Increasing Greenhouse Gases*, *Science of Climate Change*, Vol. 2.3 (2022) pp. 212-238, <https://doi.org/10.53234/scc202212/17>
  24. Roth E., 2025: *About the Origin of CO<sub>2</sub> in the Atmosphere: Some Annotations to a Study of the CO<sub>2</sub> Coalition*, *Science of Climate Change*, Vol. 5.1 (2025) prelim. pp. 1-14, <https://doi.org/10.53234/scc202501/05>
  25. Robbins B., 2025: *Atmospheric CO<sub>2</sub>: Exploring the Role of Sea Surface Temperatures and the Influence of Anthropogenic CO<sub>2</sub>*, *Science of Climate Change*, Vol. 5.1 (2025) pp. 86-102, <https://doi.org/10.53234/scc202504/23>
  26. Jaworowski Z., Segalstad T.V., Hisdal V., 1992: *Atmospheric CO<sub>2</sub> and global warming: a critical review*. 2nd edition, 1992, [https://www.researchgate.net/publication/307215789\\_Atmospheric\\_CO<sub>2</sub> and global warming a critical review 2nd edition](https://www.researchgate.net/publication/307215789_Atmospheric_CO2_and_global_warming_a_critical_review_2nd_edition)
  27. Jaworowski Z., Segalstad T.V., Ono N., 1992: *Do glaciers tell a true atmospheric CO<sub>2</sub> story?* *The Science of The Total Environment* 114(12):227-284, [https://doi.org/10.1016/0048-9697\(92\)90428-U](https://doi.org/10.1016/0048-9697(92)90428-U)
  28. Jaworowski Z., 1994: *Ancient atmosphere- Validity of ice records*, *Environ. Sci. & Pollut. Res.* 1, 161–171 (1994), <https://doi.org/10.1007/BF02986939>
  29. Schmidt G., 2024: *Climate models can’t explain 2023’s huge heat anomaly - we could be in uncharted territory*, *Nature* 627, 467 (2024), <https://doi.org/10.1038/d41586-024-00816-z>

30. Vömel H., Evan S., Tully M., 2022: *Water vapor injection into the stratosphere by Hunga Tonga-Hunga Ha’apai*. *Science* 377, 1444-1447 (2022), <https://doi.org/10.1126/science.abq2299>
31. Vinós J., Curry J., 2024: *Hunga Tonga volcano: impact on record warming*, <https://judith-curry.com/2024/07/05/hunga-tonga-volcano-impact-on-record-warming/>
32. Spencer R.: *Latest Global Temps*, <https://www.drroyspencer.com/latest-global-temperatures> Accessed on 28, August 2025
33. NOAA Microwave Sounding Temperature Assessment System: <https://www.star.nesdis.noaa.gov/smcd/emb/mscat/products.php> Accessed 29, August 2025
34. Remote Sensing Systems: [https://images.remss.com/msu/msu\\_time\\_series.html](https://images.remss.com/msu/msu_time_series.html), Accessed 29, August 2025
35. Katata G., Connolly R., O’Neill P., 2023: *Evidence of Urban Blending in Homogenized Temperature Records in Japan and in the United States: Implications for the Reliability of Global Land Surface Air Temperature Data*, *J. Appl. Meteorol. Climatol.* 2023, 62, 1095–1114. <https://doi.org/10.1175/JAMC-D-22-0122.1>
36. Spencer R.W., Christy J.R., Braswell W.D., 2025: *Urban Heat Island Effects in U.S. Summer Surface Temperature Data, 1895–2023*, *J. Appl. Meteorol. Climatol.* 2025, 64, 717–728, <https://doi.org/10.1175/JAMC-D-23-0199.1>
37. Met Office Hadley Centre observations datasets: CRUTEM.5.0.2.0 Data Download: <https://www.metoffice.gov.uk/hadobs/crutem5/data/CRUTEM.5.0.2.0/download.html> Accessed 27, August 2025
38. Osborn T.J., Jones P.D., Lister D.H., Morice C.P., Simpson I.R., Harris I.C., 2020: *Land surface air temperature variations across the globe updated to 2019: the CRUTEM5 dataset*, *J. Geophys. Res.*, <https://doi.org/10.1029/2019JD032352>
39. Met Office Hadley Centre observations datasets: HadSST.4.1.1.0 Data: download: <https://www.metoffice.gov.uk/hadobs/hadsst4/data/download.html>, Accessed 6, July 2025
40. Kennedy J.J., Rayner N.A., Atkinson C.P., Killick R.E., 2019: *An Ensemble Data Set of Sea Surface Temperature Change from 1850: The Met Office Hadley Centre HadSST.4.0.0.0 Data Set*. *Journal of Geophysical Research: Atmospheres*, 124., <https://doi.org/10.1029/2018JD029867>
41. Met Office Hadley Centre observations datasets: HadISDH.blend data download - version 1.5.1.2024f: <https://www.metoffice.gov.uk/hadobs/hadisdh/downloadBLEND.html>, Accessed 28, June 2025
42. Willett K.M., Dunn R.J.H., Thorne P.W., Bell S., de Podesta M., Parker D.E., Jones P.D., Williams Jr. C.N., 2014: *HadISDH land surface multi-variable humidity and temperature record for climate monitoring*, *Clim. Past*, 10, 1983-2006, <https://doi.org/10.5194/cp-10-1983-2014>
43. Smith A., Lott N., Vose R., 2011: *The Integrated Surface Database: Recent Developments and Partnerships*. *Bulletin of the American Meteorological Society*, 92, 704–708, <https://doi.org/10.1175/2011BAMS3015.1>
44. Willett K.M., Williams Jr. C.N., Dunn R.J.H., Thorne P.W., Bell S., de Podesta M., Jones P.D., Parker D.E., 2013: *HadISDH: An updated land surface specific humidity product for climate monitoring*. *Climate of the Past*, 9, 657-677, <https://doi.org/10.5194/cp-9-657-2013>
45. Willett K.M., Dunn R.J.H., Kennedy J.J., Berry D.I., 2020: *Development of the HadISDH marine humidity climate monitoring dataset*. *Earth System Science Data*. 12, 2853-2880, <https://doi.org/10.5194/essd-12-2853-2020>
46. Freeman E., Woodruff S.D., Worley S.J., Lubker S.J., Kent E.C., Angel W.E., Berry D.I.,

- Brohan P., Eastman R., Gates L., Gloeden W., Ji Z., Lawrimore J., Rayner N.A., Rosenhagen G., Smith S.R., 2016: *ICADS Release 3.0: A major update to the historical marine climate record*. Int. J. Climatol. 37: 2211–2232, <https://doi.org/10.1002/joc.4775>
47. NASA-GISS: Panoply Data Viewer, <https://www.giss.nasa.gov/tools/panoply/download/>, Accessed 4, July 2025
48. NASA-CERES, CERES\_EBAF-TOA\_Ed4.2.1 Subsetting and Browsing: <https://ceres-tool.larc.nasa.gov/ord-tool/jsp/EBAFTOA421Selection.jsp>, Accessed 28, August 2025
49. Loeb N.G., Doelling D.R., Wang H., Su W., Nguyen C., Corbett J.G., Liang L., Mitrescu C., Rose F.G., Kato S., 2018: *Clouds and the Earth’s Radiant Energy System (CERES) Energy Balanced and Filled (EBAF) Top-of-Atmosphere (TOA) Edition-4.0 Data Product*. J. Climate, 31, 895-918, <https://doi.org/10.1175/JCLI-D-17-0208.1>
50. Kato S., Rose F.G., Rutan D.A., Thorsen T.J., Loeb N.G., Doelling D.R., Huang X., Smith W.L., Su W., Ham S.-H., 2018: *Surface irradiances of Edition 4.0 Clouds and the Earth’s Radiant Energy System (CERES) Energy Balanced and Filled (EBAF) data product*, J. Climate, 31, 4501-4527, <https://doi.org/10.1175/JCLI-D-17-0523.1>
51. NASA-CERES, CERES\_SYN1deg\_Ed4.2 Subsetting and Browsing: <https://ceres-tool.larc.nasa.gov/ord-tool/jsp/SYN1degEd42Selection.jsp> Accessed 28, August 2025
52. Doelling D.R., Loeb N.G., Keyes D.F., Nordeen M.L., Morstad D., Nguyen C., Wielicki B.A., Young D.F., Sun M., 2013: *Geostationary Enhanced Temporal Interpolation for CERES Flux Products*, Journal of Atmospheric and Oceanic Technology, 30(6), 1072-1090., <https://doi.org/10.1175/JTECH-D-12-00136.1>
53. Doelling D.R., Sun M., Nguyen L.T., Nordeen M.L., Haney C.O., Keyes D.F., Mlynchak P.E., 2016: *Advances in Geostationary-Derived Longwave Fluxes for the CERES Synoptic (SYN1deg) Product*, Journal of Atmospheric and Oceanic Technology, 33(3), 503-521., <https://doi.org/10.1175/JTECH-D-15-0147.1>
54. NOAA Global Monitoring Laboratory: *Trends in Atmospheric Carbon Dioxide (CO<sub>2</sub>)*: [https://gml.noaa.gov/ccgg/trends/gl\\_data.html](https://gml.noaa.gov/ccgg/trends/gl_data.html), Accessed 27, August 2025
55. Lan X., Tans P. and Thoning K.W., 2025: *Trends in globally-averaged CO<sub>2</sub> determined from NOAA Global Monitoring Laboratory measurements*. Version 2025-09, <https://doi.org/10.15138/9N0H-ZH07>
56. Koutsoyiannis D., Kundzewicz Z.W., 2020: *Atmospheric Temperature and CO<sub>2</sub>: Hen - Or Egg Causality?* Sci 2020, 2(4), 83, <https://doi.org/10.3390/sci2040083>
57. Koutsoyiannis D., Onof C., Kundzewicz Z.W., Christofides A., 2023: *On Hens, Eggs, Temperatures and CO<sub>2</sub>: Causal Links in Earth’s Atmosphere*, Sci 2023, 5(3), 35; <https://doi.org/10.3390/sci5030035>
58. Kanda Y., 2013: *Investigation of the freely available easy-to-use software ‘EZR’ for medical statistics*, Bone Marrow Transplantation 2013: 48, 452–458, <https://doi.org/10.1038/bmt.2012.244>
59. Essex C., McKittrick R., Andresen B., 2007: *Does a Global Temperature Exist?*, Journal of Non-Equilibrium Thermodynamics, Volume 32, Issue 1, pp.1-27, <https://doi.org/10.1515/JNETDY.2007.001>
60. Soon W., 2025: *How well can we measure the Earth’s energy budget?*, DDP, July 5, 2025 Tucson, AZ, <https://www.youtube.com/watch?v=tI0qmV2Bbc8>, Accessed 12, July 2025

## Appendix

This appendix compiles information that, while not unrelated to the main text, is not its primary focus. And the author (Ato) has previously pointed out the origins of rising atmospheric CO<sub>2</sub> concentrations and the flaws in the reconstruction methods using polar ice cores, which form the fundamental premise of the anthropogenic CO<sub>2</sub> rise theory.

Between previous papers and the writing of this paper, the author realized that understanding the overall picture of the reality could be understood only through basic calculations (carbon isotopes) and thus decided to share this insight. And the main text presents analysis based on time difference adjustments, this approach is also applicable to the author's past research, prompting its inclusion here.

### 1. Supplemental information for the main text

#### 1.1. Regarding each temperature database and the global average temperature

This study used only UAH as the global temperature indicator. The reason is simply that, apart from UAH, there is concern about the potential for overestimation. As explained in the Materials and Methods section of the main text, besides UAH, the global temperature databases derived from meteorological satellites include NOAA-STAR [33] and RSS [34]. When comparing G-SpHm with temperature in this study, either ocean temperatures, the primary source of water vapor—or an alternative indicator, are necessary. However, RSS does not separately present land and ocean data. NOAA-STAR provides land and ocean data separately but lacks data broken down by latitude. Verifying time differences by latitude is also important.

Furthermore, as a more fundamental reason, data accuracy must also be considered. Nikolov and Zeller [17], who reported a strong correlation between temperature and albedo using 2024 NASA-CERES data, employed the global average temperature derived from non-UAH data. However, as explained in the Materials and Methods, approximately 20 % of the temperature increase observed over the past few decades in surface measurement data is most likely overestimated due to the urban heat island effect [35, 36]. RSS showed a similar warming trend to surface stations (NASA-GISS and Hadley Centre) (Figure A1, cited from their Figure 4 in [17]). At this point, RSS also needs to consider the risk of overestimation. Furthermore, NOAA-STAR data showed a trend positioned between surface data and UAH.

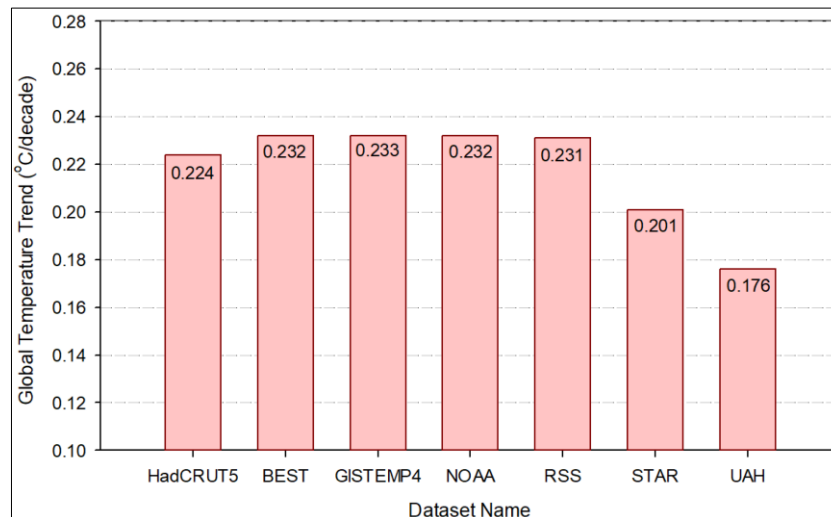


Figure A1: Temperature trend of various datasets, sited from [17]

Therefore, data from NOAA-STAR should be also considered as to the risk of overestimation. Conversely, the trend in UAH data is about 20 % lower than that of Hadley and NASA-GISS

data. Thus, from this perspective as well, UAH data has the highest objectivity. For reference, Figure A2 shows UAH, NOAA-STAR, and RSS data since 2000 [32, 33, 34].

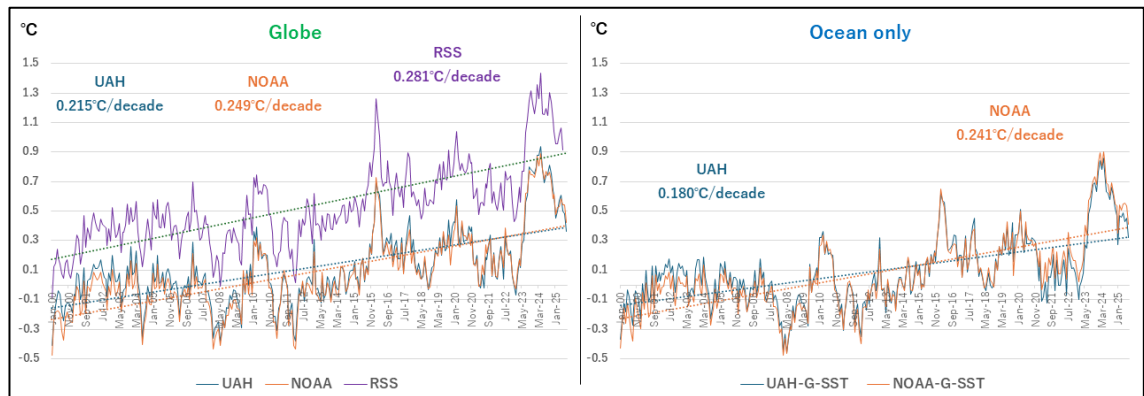


Figure A2: Temperature data from meteorological satellites. UAH and NOAA cover January 2000 to July 2025. RSS covers January 2000 to May 2025. NOAA values show the difference from the average for January 2000 to December 2019. RSS values show the difference from the average for January 1979 to December 1998.

Therefore, considering the type of data required and the fundamental accuracy of the data, UAH was selected as the sole option for this verification.

Here, the author will supplement the actual nature of the figure known as the global average temperature (GAT). Regardless of the point raised in Reference 59, it is fundamentally impossible to perfectly average physical states like temperature. Strictly speaking, temperature presupposes that within a defined range of the measured object (whether a spatial area or a specified point), the state of the gas and temperature within that range are all stable and uniformly the same.

This is possible in a laboratory setting, but impossible in the real world. For instance, temperatures observed just one meter apart can vary drastically depending on whether the area is directly exposed to sunlight or in shade. On the Earth's surface, colour alone can cause extreme variations. Averaging such conditions inherently has limitations.

However, in this age of scientific civilization, it is necessary to continuously evaluate the state of the Earth numerically, within the limits of available time and budget, starting with the highest-priority phenomena. Therefore, some benchmark is required. The same applies to the Earth's temperature. Consequently, certain rules must be established (fixed-point observations at locations minimally affected by artificial influences, over a fixed area and period), and the value obtained must be averaged. Alternatively, if more objective statistical methods exist, they should be fully utilized.

And the numerical values calculated under these consistent rules are referred to as GAT. Furthermore, in recent years, reports showing a strong correlation between the preceding GAT (and G-SST) and  $\Delta\text{CO}_2$  have been emerging one after another, regardless of the author's (Ato) report. The high correlation between UAH-G-SST and G-SpHm as shown in Figure 3, whose data are derived from independent institutes and different methods, is striking.

Moreover, not limited to this study, indicators of solar activity and global temperature indicators show a consistent correlation. These cannot be considered coincidental. Therefore, the numerical values used as a benchmark for global average temperature should be considered to have a certain degree of plausibility as an indicator for evaluating the state of the Earth. This holds true even if a certain degree of error occurs due to facilities or researchers.

### *1.2. The failure of the CO<sub>2</sub>-dependent model as demonstrated only by data from the past 10,000 years and misperceptions by Dr. Schmidt*

Figure A3 shows temperature reconstructions for the Arctic (Badgeley et al. [61]) and Antarctic

(Masson-Delmotte et al. [62]) over the past approximately 10,000 years, atmospheric CO<sub>2</sub> reconstruction data (NOAA [63], Bereiter et al. [64]), and the assumed radiative forcing due to CO<sub>2</sub> (Lightfoot and Mamer [65], Etminan et al. [66]). Temperature is represented by  $\delta^{18}\text{O}$ . Furthermore, since the data from the North Greenland Ice Core Project (NGRIP) has a temporal resolution of 20 years, making comparisons with 100 years ago easier, the change per 100 years is also shown ( $\Delta\delta^{18}\text{O}/100\text{y}$ ).

It has been reported that CO<sub>2</sub> data from ice cores prior to 1958 are grossly underestimating errors [18, 19, 26-28]. However, since modern anthropogenic CO<sub>2</sub> warming theory is based on these values, the discussion will proceed assuming these values are accurate.

As Figure A3 clearly shows, temperatures indicated by  $\delta^{18}\text{O}$  fluctuate independently of CO<sub>2</sub> concentrations and the assumed radiative forcing. The NGRIP data is provided at a 20-year time resolution, representing the average of the preceding and following 10-year periods. Therefore, it is self-evident that increasing the time resolution would reveal even greater fluctuations.

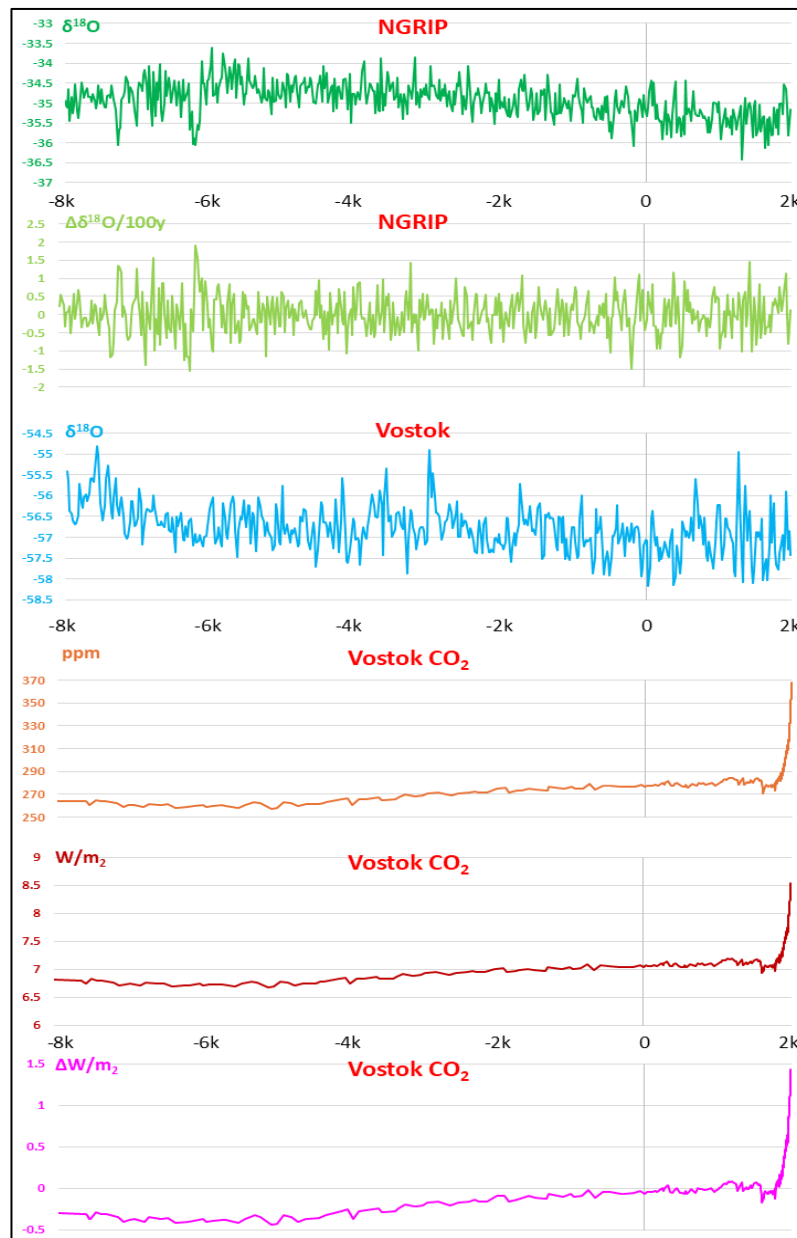
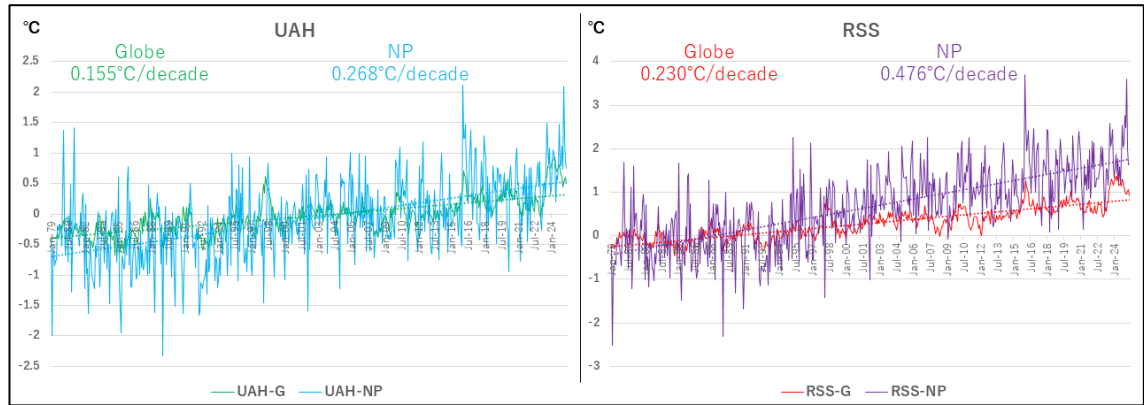


Figure A3: Climate reconstruction over the past approximately 10,000 years, with the present day (AD) at the far right.  $\delta^{18}\text{O}$  at the Arctic and Antarctic,  $\Delta\delta^{18}\text{O}$  per century in the Arctic. CO<sub>2</sub> from Antarctic ice cores and Hawaii measurements, CO<sub>2</sub> radiative forcing. NGRIP final year is 1990. Radiative forcing calculations cited from [66] (the formula is written in the Appendix 1.3).

And over the entire period, whether every 20 years or every 100 years, temperatures fluctuate by 2 to 3 degrees Celsius up or down. As shown in Figure A4, the global average is about half that of the Arctic region. Therefore, globally, temperatures constantly fluctuate by 1 to 1.5 degrees Celsius every 100 years. The IPCC critically asserts that the 20th century saw crisis warming of approximately 0.8 degrees Celsius. In reality, however, this is an unremarkable change that has been repeated countless of times throughout history. Furthermore, the so-called Medieval Warm Period around the year 1000 AD is evident. Arctic data only extends to 1990, but it shows that temperatures were significantly higher around 1940.



*Figure A4: Global and Arctic temperatures from January 2000 to May 2025 for UAH and RSS. G: Globe, NP: North Pole. The coverage areas differ: UAH-NP spans 60N to 90N, while RSS-NP spans 60N to 82.5N.*

The theory of anthropogenic global warming was recently forcefully asserted, starting in 1980s. A particular turning point came in 1988 with the press conferences held by Dr. James Hansen, Mr. Al Gore, and Mr. Timothy Worth [67]. However,  $\delta^{18}\text{O}$  data of NGRIP indicates that temperatures were not high at all at this time. The apparent rapid warming shown by surface-focused data was likely due to inadequate accounting for the urban heat island effect.

Figure A5 shows data for the last 500 years. Even around the time of the Industrial Revolution,  $\delta^{18}\text{O}$  and  $\Delta\delta^{18}\text{O}/100\text{y}$  showed earlier and more pronounced fluctuations than  $\text{CO}_2$ . While Antarctic data requires consideration of its lower temporal resolution compared to NGRIP, it shows some differences except for the steep warming in the early 20th century.

Nevertheless, these data clearly demonstrate that  $\text{CO}_2$  was not the starting point for climate change. This is because temperatures precedingly fluctuate independently of  $\text{CO}_2$ . Moreover, these realities are based on the assumption that “the age shifts of  $\text{CO}_2$  in ice cores and the modern  $\text{CO}_2$  linkage method are unquestionably valid” [19]. In other words, these global temperature changes cannot be explained by the radiative forcing of  $\text{CO}_2$  derived from Antarctic ice cores, which anthropogenic global warming proponents hold as absolute.

Therefore, climate models adopted by the IPCC, which treat  $\text{CO}_2$  as the primary factor in the greenhouse effect, cannot possibly reproduce past climates. This means that even a simple observation of paleoclimate data clearly shows that the anthropogenic  $\text{CO}_2$  warming theory and its models lack any basis from the outset. It was not a matter of mathematical modelling.

The partial agreement with some modern data achieved by models premised on anthropogenic  $\text{CO}_2$  warming is merely a pseudo-correlation resulting from cherry-picking (typically, the hockey stick curve). The rapid modern temperature rise is simply the result of connecting numerical values that fail to adequately account for the urban heat island effect, although it is a fact that there has been some warming in modern times.

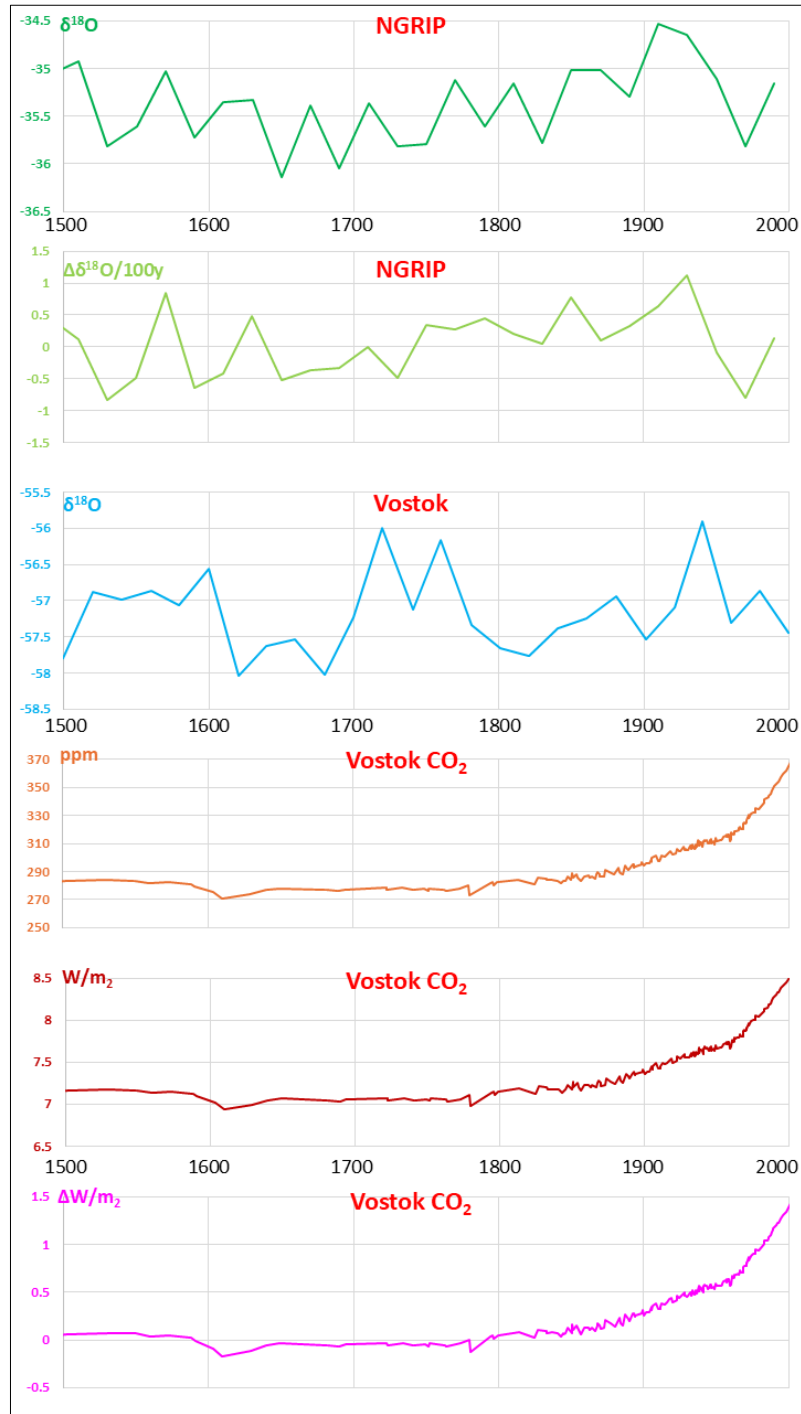


Figure A5: Climate reconstruction over the past 500 years, with modern times (AD) at the far right. Data meaning is the same as in Figure A3.

Moreover, the high temperatures in the Arctic region from the first half of the 20th century to 1940, as shown in Figures A3 and A5, also demonstrate the validity of the chemical method—one of the CO<sub>2</sub> reconstruction methods—developed by Beck (Beck [68], Harde [69]).

Furthermore, Dr. Schmidt's report [29] states that the present day may be the warmest in the last 100,000 years.

*We need answers for why 2023 turned out to be the warmest year in possibly the past 100,000 years.*

However, as shown in the two figures above, this perception itself is mistaken. Far from the

Medieval Warm Period, even the period from 1920 to 1940 was significantly warmer according to NGRIP data, and it is unlikely that the rise since 1990 could surpass it. Since the NGRIP data has a time resolution of 20 years, it is certain that there were years that were even warmer than what this data indicates.

Figure A6 illustrates typical data for the Medieval Warm Period (Keigwin [70], Robinson et al. [71,72]).

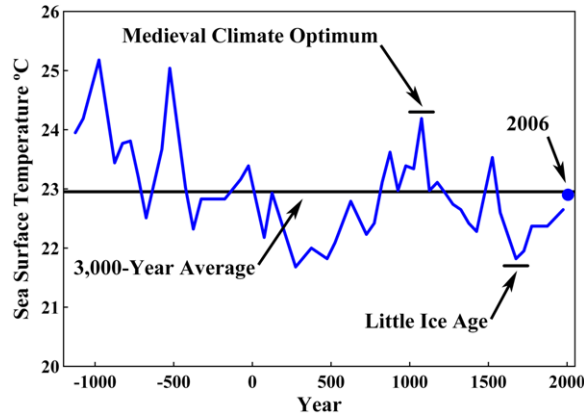


Figure A6: A typical example of the Medieval Warm Period. The Sargasso Sea. Figure from [72].

Figure A7 includes valid climate reconstruction data reproducing the Holocene Climate Optimum and Medieval Warm Period as published in the IPCC First Assessment Report (Houghton et al. [73]). It is ironic and intriguing that global temperatures in 1990, when the IPCC First Assessment Report was published, were in a completely unremarkable state.

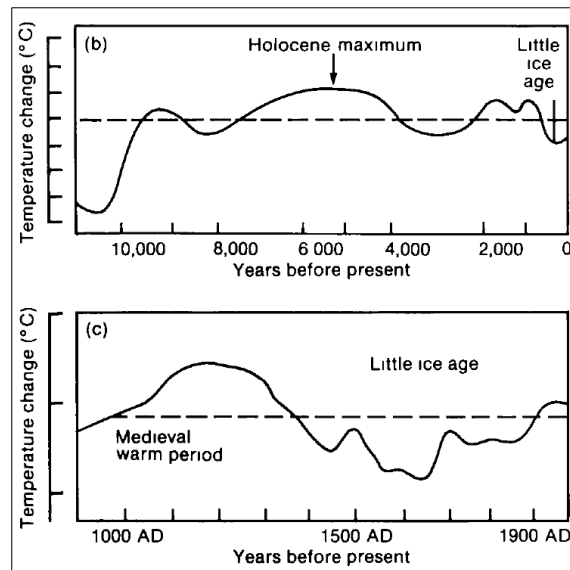


Figure A7: Reasonable climate reproduction data from the IPCC First Assessment Report. From Figure 7.1 on page 202 of [73].

Furthermore, several months ago, a natural science journal within the same Nature portfolio (Auer et al. [74]) reported that Arctic temperatures reached a maximum of 9 degrees Celsius warmer during summer than modern times during the Holocene Optimum. This equates to approximately 5 degrees Celsius globally. The relevant text is quoted here (at the beginning of P9).

*As outlined in the introduction, the former period is of particular relevance by providing a glimpse into the future, as summer surface temperatures were up to 9 °C higher than today.*

1.3. Why the results remain essentially unchanged even when atmospheric CO<sub>2</sub> data used in multivariate analysis is converted to radiative forcing

Using two representative equations employed in Appendix 1B above, CO<sub>2</sub> concentration is converted to radiative forcing (RF) using representative equations and shown in Figure A8 [65].

$$\text{Absolute value: } RF = -0.0000248 \cdot C^2 + 0.03231 \cdot C \quad (A1)$$

$$\text{Difference from 280 ppm: } \Delta RF = 5.22 \cdot \ln \frac{C}{280} \quad (A2)$$

where C is the CO<sub>2</sub> concentration (ppm) to be evaluated, and Ln is the natural logarithm.

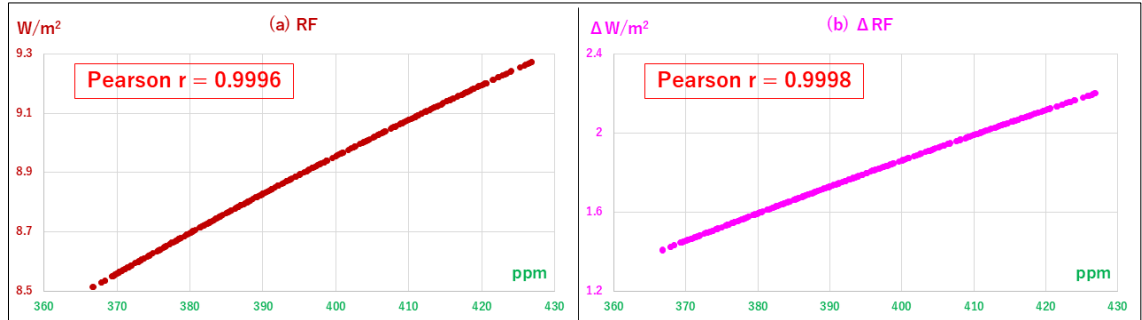


Figure A8: CO<sub>2</sub> concentration and radiative forcing since 2000. Equation adapted from [65]. (a) Actual radiative forcing (b) Difference from 280 ppm.

For both, they increase almost linearly and exhibit a correlation coefficient with CO<sub>2</sub> concentration itself that effectively shows  $r = 1$ , within the range of atmospheric CO<sub>2</sub> concentrations examined in the main text since the year 2000. Therefore, even if these radiative forcing conversion data are input as explanatory variables in multivariate analysis, the results remain essentially unchanged.

1.4. Explanation that the correlations between ASW and TSI with G-SST used in this study are not spurious

When analyzing time-series data, testing for spurious correlations is recommended. However, since ASW and TSI are fundamentally preceding G-SST, and reports supporting the so-called Svensmark effect have been accumulating, this item is presented in simplified form.

The data underlying the results of Table 5, which constitute the final result of this study, will be used.

First, scatter plots of each indicator are shown.

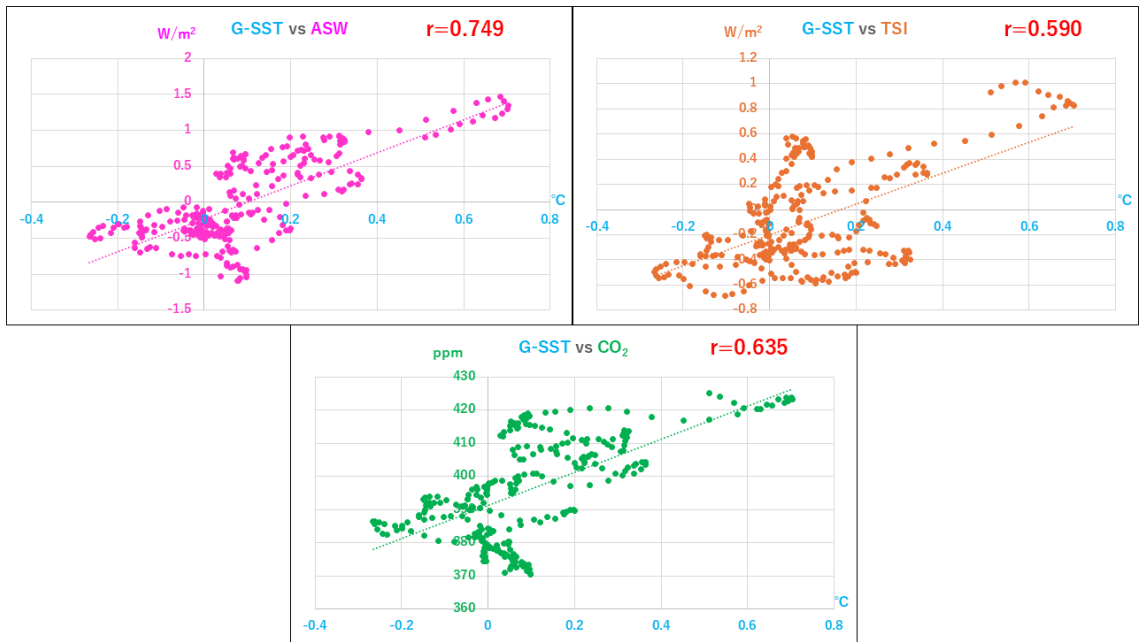


Figure A9: Scatter plots of each indicator,  $r$  = Pearson correlation, note that the data of CO<sub>2</sub> is used as is, because applying 13mRM is meaningless (the result of multivariate analysis does not essentially change).

These data show that each indicator is significantly correlated with G-SST.

Next, two correlation diagrams showing monthly changes are presented.

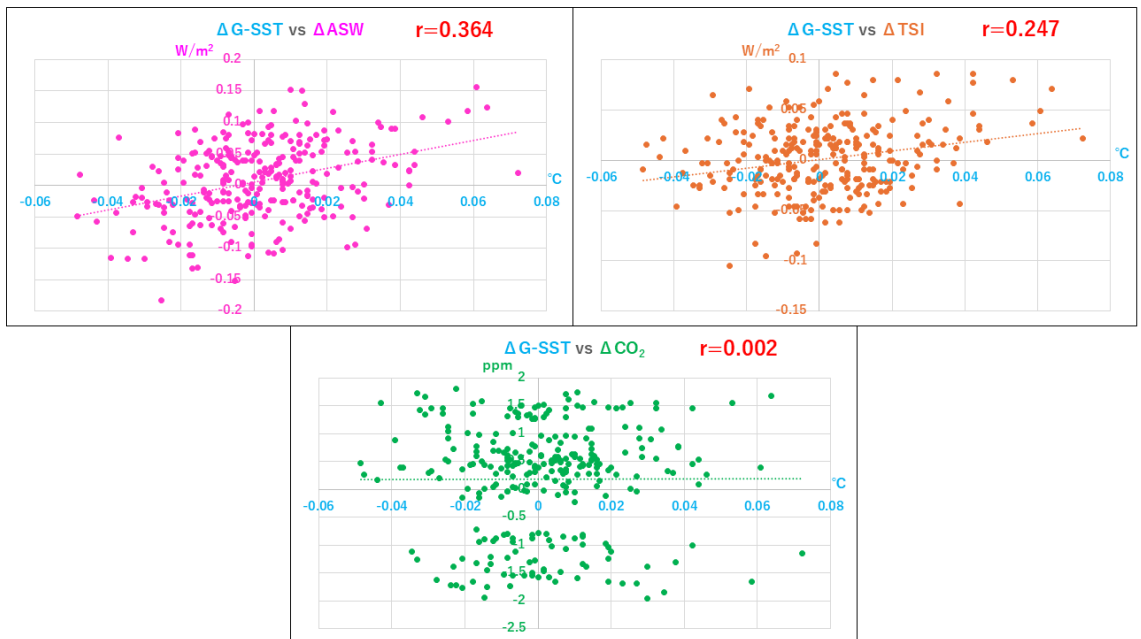


Figure A10: Scatter plots of monthly change of each indicator,  $r$  = Pearson correlation

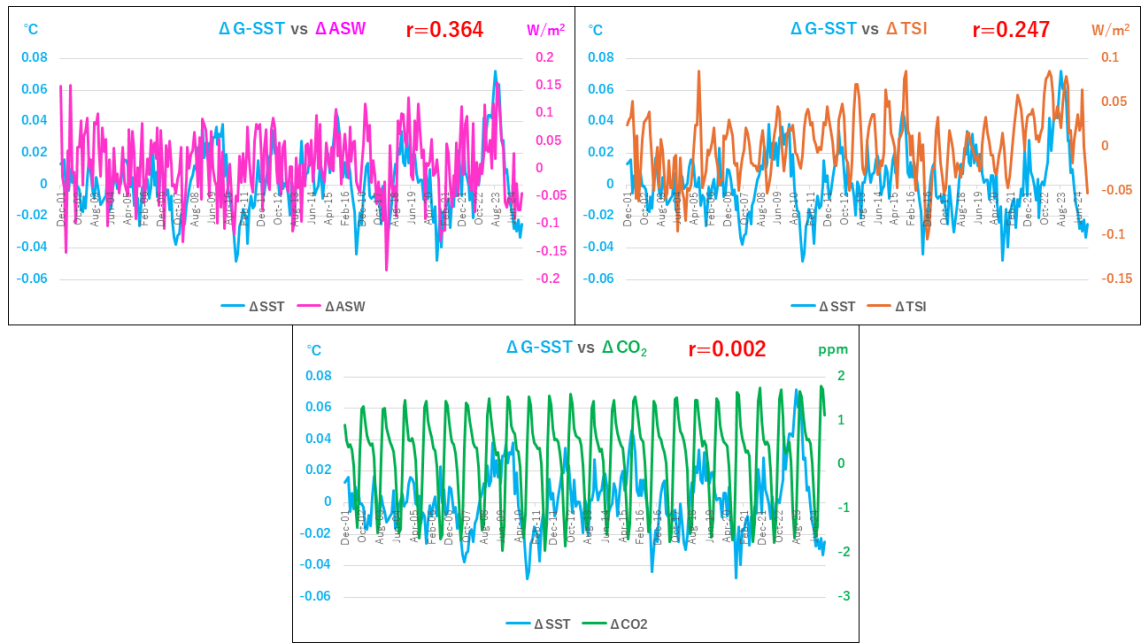


Figure 11A: Time series plotting of monthly change of each indicator,  $r$  = Pearson correlation

As evident from both the scatter plot and time-series data, there is no correlation between  $\Delta G$ -SST and  $\Delta CO_2$ . Therefore, it is clear that G-SST and  $CO_2$  were spuriously correlated. On the other hand,  $\Delta ASW$  and  $\Delta TSI$  are significantly correlated with  $\Delta G$ -SST.

Finally, the result of the linear multiple regression analysis with  $\Delta G$ -SST as the dependent variable is presented.

Table A1: Multiple linear regression analysis of  $\Delta G$ -SST as an objective variable

Model $R^2=0.171$ $P=4.44e-11$	Regression Coefficient	P
Constant	0.00077	0.49
$\Delta ASW$	0.11016	5.8e-09
$\Delta TSI$	0.11354	4.6e-04
$\Delta CO_2$	-0.00025	0.825

$\Delta ASW$  and  $\Delta TSI$  were independent determinants of  $\Delta G$ -SST, but  $\Delta CO_2$  and the constant were not. Therefore, it is reasonable to conclude that ASW and TSI exhibit a genuine correlation with G-SST at least within the scope of this data set.

## 2. Understanding the origin of atmospheric CO<sub>2</sub> increase by a concept of simple math using average of $\delta^{13}C$

This section is designed to help even those unfamiliar with science grasp the overall picture of past carbon cycles through basic mathematical calculations. While rigorous verification already exists, exemplified by Koutsoyiannis [21], not everyone can fully comprehend scientific papers.

Those who attribute all the rise in atmospheric CO<sub>2</sub> today to human origins, whether researchers or the general people—frequently claim this is proven by carbon isotope ratios. This is because, especially since the Industrial Revolution, the <sup>13</sup>C ratio has decreased and appears to correlate with the increase of atmospheric CO<sub>2</sub> concentrations and human emissions. However, this claim can be proven false with a basic elementary-level numerical check.

Let us suppose CO<sub>2</sub> levels at the start of the Industrial Revolution were 280 ppm, and the increase up to 2022 was 140 ppm. Let us suppose δ<sup>13</sup>C at the start of the Industrial Revolution was -6.3 ‰, and the δ<sup>13</sup>C of anthropogenic CO<sub>2</sub> is -26 ‰ (because fossil fuels, primarily C<sub>3</sub> plants, have significantly lower <sup>13</sup>C content).

It is simply a matter of taking these averages.

$$\{(-6.3 \times 280) + (-26 \times 140)\} \div 420 = -12.86666\dots \quad (A3)$$

If the entire 140 ppm increase were anthropogenic, δ<sup>13</sup>C should have been approximately -12.87 ‰ by the end of 2022.

However, the actual atmospheric δ<sup>13</sup>C is around -8.4 ‰ (2022). Therefore, it is impossible to attribute the entire 140 ppm increase solely to human activity.

Thus far, using the basic mathematical concept of calculating averages is explained. This explanation should suffice for gaining a simple understanding of the actual situation described in this series of points.

Naturally, similar results are reproduced using the precise definition of δ<sup>13</sup>C (Lueker et al. [75]) and calculations. The details are explained in the following two slides.

Calculation by the definition of δ<sup>13</sup>C

\* definition1: standard of carbon isotope, <sup>13</sup>C/<sup>12</sup>C = R<sub>s</sub> = 13C<sub>s</sub>/12C<sub>s</sub> = 0.0112372  
 \* definition2: δ<sup>13</sup>C = (<sup>13</sup>C/<sup>12</sup>C - R<sub>s</sub>) ÷ R<sub>s</sub> = (<sup>13</sup>C/<sup>12</sup>C - 0.0112372) ÷ 0.0112372  
 \* supposition1: CO<sub>2</sub> = 280ppm in 1750, δ<sup>13</sup>C = -0.0063 (or -6.3‰)  
 \* supposition2: increased 140ppm of CO<sub>2</sub>, δ<sup>13</sup>C = -0.026 (or -26.0‰)

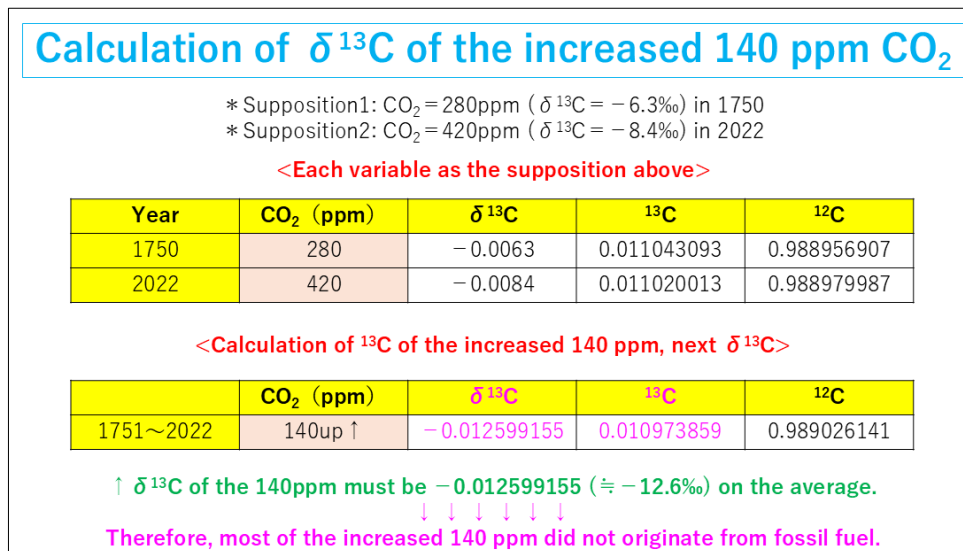
Year	ppm	<sup>13</sup> C/ <sup>12</sup> C	δ <sup>13</sup> C
1750	280	0.011166406	-0.0063
1751~2022	140up ↑	0.010945033	-0.026
2022	420	0.011092604	-0.012867624

\* If the 140-ppm increase is all man-made,  
δ<sup>13</sup>C in 2022 must be -0.012867624 (≠ -12.9‰)

*Slide A1: Explanation using carbon isotope. Calculation, supposing the entire 140-ppm increase is anthropogenic.*

The content of Slide A1 above shows the calculation process for atmospheric δ<sup>13</sup>C in 2022, assuming δ<sup>13</sup>C = -26 ‰ for 140-ppm increase and that all of this is accumulated. As shown in the final result, δ<sup>13</sup>C ≈ -12.87 ‰, which shows no substantial difference from the simple average calculation method described above. However, in reality, the δ<sup>13</sup>C value for modern atmospheric CO<sub>2</sub> is approximately -8.4 ‰.

The content of the next slide A2 shows the back-calculation process for the 140-ppm increase in δ<sup>13</sup>C, derived from δ<sup>13</sup>C values during the Industrial Revolution and modern reality. The result indicates that δ<sup>13</sup>C of 140 ppm was ≅ -12.6 ‰. Therefore, it is impossible to claim that the 140-ppm increase is entirely anthropogenic.



Slide A2: Explanation using carbon isotope. Back-calculated  $\delta^{13}\text{C}$  of the 140-ppm increase from the  $\delta^{13}\text{C}$  values of the past and present.

However, at this stage, another possibility for the 140-ppm increase cannot be ruled out. Amid rising anthropogenic emissions, it is possible that while the quantitative increase is anthropogenic in origin, the composition has been replaced by natural cycles, leading to the current state. The results of multivariate analysis presented in the author's two previous papers [18,19] quantitatively and probabilistically determined the veracity of this possibility. The hypothesis itself—that human emissions and land-use changes caused the CO<sub>2</sub> rise over the past 60-plus years—was shown to be statistically highly improbable. Therefore, even today, most of the atmospheric CO<sub>2</sub> rise is assertively a natural phenomenon.

And as this explanation shows, the discrepancy between the anthropogenic theory of global warming and CO<sub>2</sub> rise and the reality arises precisely because of the assumption that the CO<sub>2</sub> values reproduced from ice cores are the truth.

Furthermore, if one possesses the knowledge to understand the explanations accompanying the two slides above, it is unlikely they would unquestioningly accept the anthropogenic theory of CO<sub>2</sub> rise itself. Therefore, it is recommended that the content of this supplement be used solely for the purpose of explaining the initial explanation (verification based on the concept of averages) to those with limited scientific knowledge.

### 3. Multivariate analysis considering the time lag between temperature and annual atmospheric CO<sub>2</sub> increase ( $\Delta\text{CO}_2$ ) of author’s previous reports

In the author's previous multivariate analyses [18, 19], only annual values were used. The results rejected the anthropogenic theory for  $\Delta\text{CO}_2$ , with SST being the sole determinant. However, as demonstrated above in this report, there is a consistent time lag between actual global surface temperature and  $\Delta\text{CO}_2$ . Therefore, analysis using monthly data would be ideal.

Yet, anthropogenic emissions data commonly available from institutions like the International Energy Agency and Our World in Data (OWID) are not monthly. Regarding temperature data, however, it is easy to adjust the months, calculate annual averages, and verify the monthly difference yielding the best correlation with  $\Delta\text{CO}_2$ .

This time, using this method, G-SST was calculated using only UAH data and multivariate analysis was performed only for the period after 1980. Note that while UAH data is publicly available from December 1978 onwards, the reason for starting from 1980 is because it becomes impossible to start from 1979 in the monthly correction process, if the starting month for the annual average

G-SST is moved further back in time. Only OWID data [76] was used for anthropogenic emissions.

At the end of this section, the author's perspective on which global temperature indicators should be used in the multiple linear regression analysis with  $\Delta\text{CO}_2$  as the dependent variable will be explained.

Table A2 shows the results of linear multiple regression analysis. The optimal monthly G-SST correction was achieved by advancing the data by two months (using the average of March 1980 to February 1981 as the annual G-SST for 1980). Analysis using same-month G-SST is also shown for comparison. The model accuracy is comparable for all data combinations. However, for the combination of same-month G-SST and LUC, the constant decreases slightly and the P-value increases.

*Table A2: Results of multiple linear regression analysis with annual  $\Delta\text{CO}_2$  as the dependent variable. Data from 1980 to 2023 were analyzed. Statistically significant factors are marked in red based on multivariate analysis.  $\Delta\text{CO}_2$  data were obtained on the same date as in the main text. Emissions data were obtained from OWID, with units in megatons [76]. Pearson Correlation is with  $\Delta\text{CO}_2$ . FFO; fossil fuel only, LUC; including land use change.*

G-SST	Human Emission	Variables	Pearson correlation	Regression coefficient	P	Model R <sup>2</sup>
G-SST month adjusted	FFO	Constant ppm	---	1.86	2.76e-05	0.631 P=1.33e-09
		G-SST ppm/°C	0.793	2.35	1.98e-06	
		Human Emission ppm/Mt	0.596	6.25e-06	0.645	
	LUC	Constant ppm	---	1.78	6.36e-04	0.632 P=2.71e-08
		G-SST ppm/°C	0.793	2.33	2.07e-06	
		Human Emission ppm/Mt	0.598	7.57e-06	0.594	
G-SST same month	FFO	Constant ppm	---	1.70	8.83e-05	0.611 P=3.93e-09
		G-SST ppm/°C	0.777	2.17	6.03e-06	
		Human Emission ppm/Mt	0.596	1.20e-05	0.372	
	LUC	Constant ppm	---	1.57	1.93e-3	0.613 P=3.58e-09
		G-SST ppm/°C	0.777	2.14	5.93e-06	
		Human Emission ppm/Mt	0.598	1.39e-5	0.321	

Table A3 shows the total  $\Delta\text{CO}_2$  values and the total predicted  $\Delta\text{CO}_2$  values from this multiple regression analysis. In previous reports, verification using UAH data since 1979 showed a difference of approximately 14 ppm in the final year. In this verification, the difference was reduced to about 8 ppm using a model with FFO emissions and monthly-adjusted G-SST. Conversely, the combination of unadjusted G-SST and LUC resulted in a discrepancy of approximately 20 ppm. This outcome clearly reflects the combined effect of smaller coefficient and constant for G-SST in this model.

*Table A3: Sum of published  $\Delta\text{CO}_2$  values and sum of predicted  $\Delta\text{CO}_2$  values from the multiple regression analysis in Table A1. Units are ppm.*

	Published value	Month of G-SST	FFO	LUC
Sum of $\Delta\text{CO}_2$	84.98	Adjusted	77.30	74.00
		Same	70.22	64.79

More precise results are anticipated once detailed monthly anthropogenic emission data becomes available. However, defining monthly  $\Delta\text{CO}_2$  and implementing monthly adjustments will also become critical in that process.

Multivariate analyses with  $\Delta\text{CO}_2$  as the object variable have been conducted in three papers, including this paper. Human emissions have been included in all results tables. If these linear multiple regression analyses were performed using stepwise selection (whether Akaike Information Criteria (AIC), BIC, or p-value methods), anthropogenic emissions would be excluded from the explanatory factors, reconstructing the model to use only SST as the explanatory variable. Therefore, in this case, a nearly perfect prediction equation can be derived for the SST of any facility. However, since there are only two explanatory variables, the significance of performing stepwise regression is questionable. Consequently, the author (Ato) basically does not perform stepwise regression for this topic in his reports.

Finally, which temperature indicators in the climate research field should be used for analysis and the reasons for doing so will be described. While it depends on the objective, if the indicators have clear underlying mechanisms, they should be used. And of course, accuracy is also an important factor.

Especially with UAH data, there is no significant difference globally compared to SST regarding monthly fluctuation (Pearson  $r = 0.977$ , Dec-78 to Jun-25, as implied in Figure 1(b) which compares SST and LST, and because the ocean dominates about 70 % surface of the earth), so approximate results can be obtained (of course, decadal trend is slightly different). Furthermore, as noted in the Discussion section, the results of the multiple regression analysis with ASW and TSI as explanatory variables were equivalent regardless of whether the dependent variable was G-SST or Global temperature.

However, in the multivariate analysis the author has conducted in the previous two papers [18,19],  $\Delta\text{CO}_2$  is the objective variable, and SST is the mechanism that is clearly understood. Furthermore, for the primary purpose of this report, using ocean temperature—the source of water vapor—as the primary variable is theoretically most appropriate. Furthermore, surface data other than UAH may be subject to concerns regarding the urban heat island effect or numerically approximated errors.

Moreover, compared to UAH, other datasets generally show larger differences between ocean and land surfaces. Finally, when performing multiple linear regression analysis with  $\Delta\text{CO}_2$  as the dependent variable and extending the analysis further back in time (to 1959, due to issues with ice core data prior to 1958, as explained in [19]), it is desirable to use SST, which exhibits a relatively similar trend, for comparison with UAH and other facility data (especially for verification extending back to 1959).

Now, regarding the overall picture of Earth's carbon cycle, the ratio between land and ocean is roughly 4 to 3 (NASA, [77]). Therefore, the possibility that the actual impact could be distinguished as approximately 4 to 3 between land and ocean remains, if assuming there are no multicollinearity issues in the multiple linear regression analysis and the annual balance on land can be accurately measured. That is, the ratio would be slightly more than half of  $\Delta\text{CO}_2$  attributable to land temperature and the remainder to ocean temperature.

However, in actual linear multiple regression analysis, using highly correlated indicators as explanatory variables leads to problems (cancellation) due to multicollinearity. Moreover, since precise annual figures for the terrestrial carbon cycle are unknown, performing principal component analysis to circumvent multicollinearity is impossible.

SST precedes LST in Earth's surface temperature and dominates it to a certain extent. Oceans cover 70 % of the Earth's surface. Therefore, considering the perspective of comparing facility-specific data as mentioned above, it is most appropriate to use G-SST alone as the representative indicator of global temperature in multiple linear regression analysis with  $\Delta\text{CO}_2$  as the objective variable.

Regarding the overall carbon cycle, it is likely reasonable to consider that in tropical regions, CO<sub>2</sub>

emissions from both the ocean and land (especially soil respiration) exceed absorption (Salby and Harde, [23]), while in mid-latitude to polar ocean areas, the ocean absorbs CO<sub>2</sub>, with these cycles occurring globally. Considering that the oceans, covering 70 % of the Earth's surface, act as a ‘gravitational’ force to regulate this overall system would be currently the most reasonable perspective.

## References for Appendix

61. Badgeley J.A., Steig E.J., Hakim G.J., Fudge T.J., 2020: *Reconstructions of mean-annual Greenland temperature and precipitation for the past 20,000 years and the ice-core records used to create the reconstructions 2020*. Arctic Data Center. <https://doi.org/10.18739/A2599Z26M>  
Accessed 31, January 2025
62. Masson-Delmotte V., Buiron D., Ekaykin A.A., Frezzotti M., Gallée H., Jouzel J., Krinner G., Landais A., Motoyama H., Oerter H., Pol K., Pollard D., Ritz C., Schlosser E., Sime L.C., Sodemann H., Stenni B., Uemura R., Vimeux F., 2011: *Water stable oxygen isotope records from six Antarctic ice core sites for the present and last interglacial periods* [dataset publication series]. PANGAEA, <https://doi.org/10.1594/PANGAEA.785228>, Accessed 9, March 2025
63. NOAA, National Centers for Environmental Information: *Antarctic Ice Cores Revised 800KYr CO<sub>2</sub> Data*, <https://www.ncei.noaa.gov/access/paleo-search/study/17975>, Accessed 24, September 2024
64. Bereiter B., Eggleston S., Schmitt J., Nehrbass-Ahles C., Stocker T.F., Fischer H., Kipfstuhl S., Chappellaz J., 2015: *Revision of the EPICA Dome C CO<sub>2</sub> record from 800 to 600 kyr before present*. Geophysical Research Letters, 42(2), 542-549. <https://doi.org/10.1002/2014GL061957>
65. Lightfoot H.D., Mamer O.A., 2014: *Calculation of Atmospheric Radiative Forcing (Warming Effect) of Carbon Dioxide at Any Concentration*. Energy & Environment, 25(8), 1439-1454. <https://doi.org/10.1260/0958-305X.25.8.1439>
66. Etminan M., Myhre G., Highwood E.J., Shine K.P., 2016: *Radiative forcing of carbon dioxide, methane, and nitrous oxide: A significant revision of the methane radiative forcing*, Geophys. Res. Lett., 43, 12,614–12,623, <https://doi.org/10.1002/2016GL071930>
67. Center for Science and Technology Policy Research, 2010: *The Climate Fix: What Scientists and Politicians Won't Tell You About Global Warming*, [https://sciencepolicy.colorado.edu/publications/special/climate\\_fix/book\\_clips.html](https://sciencepolicy.colorado.edu/publications/special/climate_fix/book_clips.html)
68. Beck E.G., 2022: *Reconstruction of Atmospheric CO<sub>2</sub> Background Levels since 1826 from direct measurements near ground*, Science of Climate Change, Vol 2.2 (2022) pp.148-211, <https://doi.org/10.53234/scc202112/16>
69. Harde H., 2023: *About Historical CO<sub>2</sub>-Data since 1826: Explanation of the Peak around 1940*, Science of Climate Change, Vol. 3.2 (2023) pp. 211-218, <https://doi.org/10.53234/scc202304/21>
70. Keigwin L.D., 1996: *The Little Ice Age and Medieval Warm Period in the Sargasso Sea*. Science 274,1504-1508, <https://doi.org/10.1126/science.274.5292.1504>
71. Robinson A.B., Robinson N.E., Soon W., 2007: *Environmental Effects of Increased Atmospheric Carbon Dioxide*, Journal of American Physicians and Surgeons (2007) 12, 79-90., <https://www.jpands.org/vol12no3/robinson.pdf>
72. Oregon Institute of Science and Medicine: *Global Warming Petition Project*, [http://www.petitionproject.org/review\\_article.php](http://www.petitionproject.org/review_article.php)
73. Houghton J.T., Jenkins G.J., Ephraums J.J., IPCC, 1990: *The IPCC Scientific Assessment*, Science of Climate Change <https://scienceofclimatechange.org>

*Report Prepared for IPCC by Working Group I*, [https://www.ipcc.ch/site/assets/uploads/2018/03/ipcc\\_far\\_wg\\_I\\_full\\_report.pdf](https://www.ipcc.ch/site/assets/uploads/2018/03/ipcc_far_wg_I_full_report.pdf)

74. Auer A.G., van der Bilt W.G.M., Schomacker A., Bakke J., Støren E.W.N., Buckby J.M., Cederstrøm J.M., van der Plas S., 2025: *Hydroclimate intensification likely aided glacier survival on Svalbard in the Early Holocene*. *Commun Earth Environ* 6, 100 (2025)., <https://doi.org/10.1038/s43247-025-02064-z>
75. Lueker T., Keeling R., Bollenbacher A., Walker S., Morgan E., Brooks M., 2020: *Calibration Methodology for the Scripps 13C/12C and 18O/16O stable Isotope program 1992-2018*. UC San Diego: Scripps Institution of Oceanography. <https://escholarship.org/uc/item/4n93p288>
76. Data on CO<sub>2</sub> and Greenhouse Gas Emissions by Our World in Data, <https://github.com/owid/co2-data> Accessed 12, September 2025
77. NASA earth observatory: *The Carbon Cycle*, <https://earthobservatory.nasa.gov/features/CarbonCycle>